

BOOK OF ABSTRACTS

**Conference on Photoacoustic and
Photothermal Theory and Applications**

25-27 September 2013, Warsaw (Poland)

ORGANIZING COMMITTEE

Tomasz Starecki (conference chair)
Mariusz Suchenek
Katarzyna Opalska
Antonina Geras

Barbara Kozielska
Patrycja Hojczyk

SCIENTIFIC COMMITTEE

Darryl P. Almond
Stephen Bialkowski
Dane Bicanic
Zoltán Bozóki
Gerd Busse
Mihai Chirtoc
Gerald Diebold
Danièle Fournier
Mladen Franko
Christ Glorieux
Vitali Gusev
Peter Hess
Jyrki Kauppinen
Andreas Mandelis
Antonio Manzanares
John F. McClelland
Kirk H. Michaelian
András Miklós
Kumar Patel
Josef Pelzl
Markus Sigrist
Veronica Slezak
Masahide Terazima
Frank K. Tittel
Dragan M. Todorović
Lihong V. Wang
Shu-yi Zhang
Vladimir Zharov

Zbigniew Bielecki
Jerzy Bodzenta
Alina Dudkowiak
Miroslaw Maliński
Janusz Ryczkowski
Tomasz Starecki
Zbigniew Suszyński
Janusz Szurkowski

CONFERENCE PROGRAM

WEDNESDAY (25.09)	
8:30 – 8:55	Registration
9:00 – 9:20	Conference opening ceremony
9:20 – 10:20	Photoacoustic spectroscopy in gas sensing and biomedical applications Marcus Sigrist (keynote speech)
10:20 – 10:40	Laser photoacoustic method in dendrochronology: 300-years CO ₂ chronology of annual tree rings Yu.N. Ponomarev
10:40 – 11:00	Sensing mechanical properties of rocks and sediments by means of optoacoustics while drilling oil and gas boreholes S.V. Egerev
11:00 – 11:30	Coffee break
11:30 – 11:50	Single frequency, compact, nested cavity optical parametric oscillators in the 3.3–3.7 μm range: principle and potential for photoacoustic spectroscopy applications J.M. Melkonian
11:50 – 12:10	Photoacoustic spectroscopy of improvised explosive device precursors A. Puiu
12:10 – 12:30	Photoacoustic cell with digital differential detection M. Suchenek
12:30 – 12:50	Photoacoustic signal generation in acoustic resonators by periodic trains of laser pulses A. Miklós
12:50 – 13:10	Photoacoustic discrimination of optical absorbers based on non-linear generation E. Bossy
13:10 – 14:30	Lunch
14:30 – 15:30	Laser-based guided ultrasonic bulk (3D), surface (2D), and wedge (1D) waves in (non)destructive evaluation: from macroscopic properties to nanoscopic models Peter Hess (plenary / invited speech)
15:30 – 16:00	Coffee break
16:00 – 17:40	Poster session

THURSDAY (26.09)	
9:00 – 10:00	High frequency photoacoustic transients generated at surfaces Gerald Diebold (plenary / invited speech)
10:00 – 10:20	Dual channel diode laser spectrometer with ring type photoacoustic detector for high resolution spectroscopy and gas analysis Yu.N. Ponomarev
10:20 – 10:40	Investigation of thermal properties of SiC ceramics containing carbon nanostructures by photothermal measurements A. Kaźmierczak-Bałata
10:40 – 11:00	Laser-induced wavefront distortion in optical materials L.C. Malacarne
11:00 – 11:30	Coffee break
11:30 – 11:50	Photoacoustic imaging of defects in MEMS N. Chigarev
11:50 – 12:10	Mid-Infrared semiconductor laser based trace gas sensor technologies and applications: state-of-the-art and grand challenges F.K. Tittel
12:10 – 12:30	Wavelength dependent optical absorption of atmospheric aerosol measured by multi-wavelength photoacoustic spectrometer: a laboratory and a field study Z. Bozóki
12:30 – 12:50	A miniaturized photoacoustic gas sensor fully integrated in Si technology J. Rouxel
12:50 – 13:10	Differential open photoacoustic Helmholtz cell T. Starecki
13:10 – 14:30	Lunch
14:30 – 15:30	Advances in thermal lens microscopy for detection in microfluidic systems Mladen Franko (plenary / invited speech)
15:30 – 16:00	Coffee break
16:00 – 16:20	Photodeflection signal formation in photothermal experiments: comparison of existing theoretical description and their application to determination of thermo-optical and structural parameters of TiO ₂ based thin films D. Korte
16:20 – 16:40	Advantages and disadvantages of thermal measurements using spatial modulation technique Z. Suszyński
16:40 – 17:00	Applications of photoacoustic resonances for soft matter characterization S. Galović
17:40 – 20:30	Gala dinner

FRIDAY (27.09)	
9:00 – 10:00	Thermal wave measurements at the nanoscale Josef Pelzl (keynote speech)
10:00 – 10:20	Study on photoacoustic technique of thermophysical properties of human skin A. Yoshida
10:20 – 10:40	Photoacoustic spectroscopy based dual channel hygrometer for airborne applications D. Tatrai
10:40 – 11:00	Photoacoustic detection of NH ₃ by means of a differential double resonator cell A. Vallespi
11:00 – 11:30	Coffee break
11:30 – 11:50	Direct estimate of cocoa powder in cakes: colorimetry and photoacoustic approach O. Dóka
11:50 – 12:10	Direct quantification of carotenoids in low fat baby foods via laser photoacoustics and colorimetric index a* Gy. Végvári
12:10 – 12:30	Photoacoustic signal formation in heterogeneous multi-layered systems with piezoelectric detection M.V. Isaiev
12:30 – 12:50	Complementary photothermal techniques for complete thermal inspection of solids D. Dadarlat
12:50 – 13:10	Photothermal measurements by the use of scanning thermal microscope J. Bodzenta
13:10 – 14:30	Lunch
14:30 – 15:30	Photothermal mirror (reflection lens) of glasses and glassy materials Stephen Bialkowski (plenary / invited speech)
15:30 – 16:00	Coffee break
16:00 – 16:20	Laser ultrasonic technique in diamond anvil cell combined with optical polarimetry N. Chigarev
16:20 – 16:40	Photothermoelastic characterisation of a tuning fork used in infrared and photoacoustic spectroscopy M. Spajer
16:40 – 17:00	Photoacoustic elastic bending method: study of the microcantilevers D.M. Todorović
17:00 – 17:20	Conference closing

TABLE OF CONTENTS

PREFACE

12

KEYNOTE SPEECHES

<i>Photoacoustic spectroscopy in gas sensing and biomedical applications</i> M.W. Sigrist, J.M. Rey, J. Kottmann	13
<i>Thermal wave measurements at the nanoscale</i> J. Pelzl	14

PLENARY / INVITED TALKS

<i>Photothermal mirror (reflection lens) of glasses and glassy materials</i> S.E. Bialkowski, G.V.B. Lukasiewicz, N.G.C. Astrath	16
<i>High frequency photoacoustic transients generated at surfaces</i> B. Wu, C. Frez, G.J. Diebold	17
<i>Laser-based guided ultrasonic bulk (3D), surface (2D), and wedge (1D) waves in (non)destructive evaluation: from macroscopic properties to nanoscopic models</i> P. Hess, A.M. Lomonosov	18
<i>Advances in thermal lens microscopy for detection in microfluidic systems</i> M. Liu, M. Franko	19

THEORETICAL CONSIDERATIONS

<i>Photodeflection signal formation in photothermal experiments: comparison of existing theoretical description and their application to determination of thermo-optical and structural parameters of TiO₂ based thin films</i> D. Korte, M. Franko	21
<i>Laser-induced wavefront distortion in optical materials</i> L.C. Malacarne, N.G.C. Astrath	22

<i>Time reversal for PAT in thermo-viscous media based on the wave equation of Nachman, Smith and Waag</i>	
R. Kowar	23
<i>Finite sample size effect in laser induced surface displacement</i>	
V.S. Zanuto, L.S. Herculano, G.V.B. Lukasiewicz, L.C. Malacarne, M.L. Baesso, C. Jacinto, N.G.C. Astrath	23
<i>Single theory of electro-pyroelectric and photo-pyroelectric methods for physical properties investigation</i>	
A. Mami, I. Mellouki, N. Yacoubi	24
<i>TLM thermal modeling</i>	
Z. Suszyński	25
<i>Model of the photoacoustic Helmholtz resonator with conical ended duct</i>	
M. Suchenek	25

INSTRUMENTATION AND METHODOLOGY

<i>Photoacoustic signal generation in acoustic resonators by periodic trains of laser pulses</i>	
A. Miklós, M.G. da Silva, J. Angster	26
<i>Differential open photoacoustic Helmholtz cell</i>	
T. Starecki, A. Geras	27
<i>Parametric analysis of a differential photoacoustic Helmholtz cell</i>	
A. Geras, T. Starecki	28
<i>Improved photoacoustic generator</i>	
T. Borowski, M. Suchenek, A. Burd, T. Starecki	29
<i>Photoacoustic cell with digital differential detection</i>	
M. Suchenek	29
<i>A novel method of a photoacoustic cell frequency response evaluation</i>	
M. Suchenek	30
<i>Photoacoustic spectroscopy using a MEMS microphone with Inter-IC sound digital output</i>	
H. Bruhns, A. Marianovich, M. Wolff	30
<i>Multichannel detection of photoacoustic signals</i>	
T. Starecki, P. Zbysiński	31

SPECTROSCOPY, APPLICATIONS IN CHEMISTRY

<i>Photoacoustic detection of NH₃ by means of a differential double resonator cell</i>	
A. Vallespi, V. Slezak, A. Peuriot, F. González, A. Pereyra, G. Santiago	33

<i>Single frequency, compact, nested cavity optical parametric oscillators in the 3.3–3.7μm range: principle and potential for photoacoustic spectroscopy applications</i>	
J. Barrientos Barria, J.M. Melkonian, M. Raybaut, J.B. Dherbecourt, A. Godard, M. Lefebvre	34
<i>Mid-Infrared semiconductor laser based trace gas sensor technologies and applications: state-of-the-art and grand challenges</i>	
F.K.Tittel, R. Lewicki, M. Jahjah, P. Stefański, J. Tarka, W. Jiang, J. Zhang, L. Gong, R. Griffin, S. So, D. Thomazy, P. Lane, R. Talbot	36
<i>Determination of the singlet oxygen generation efficiency of dyes by applying absorption and optoacoustic spectroscopies</i>	
M. Kotkowiak, E. Robak, A. Dudkowiak	37
<i>Wavelength dependent optical absorption of atmospheric aerosol measured by multi-wavelength photoacoustic spectrometer: a laboratory and a field study</i>	
N. Utry, T.Ajtai, Á. Filep, Z. Bozóki, G. Szabó	38
<i>Dual channel diode laser spectrometer with ring type photoacoustic detector for high resolution spectroscopy and gas analysis</i>	
Yu.N. Ponomarev, V.A. Kapitanov	39
<i>Investigation of the photobleaching process of eosin Y in aqueous solution by thermal lens spectroscopy</i>	
L.S. Herculano, L.C. Malacarne, N.G.C. Astrath	40
<i>Photoacoustic spectroscopy of improvised explosive device precursors</i>	
A. Puiu, G. Giubileo, A. Palucci	41

SENSORS, ACTUATORS AND INDUSTRIAL APPLICATIONS

<i>Sensing mechanical properties of rocks and sediments by means of optoacoustics while drilling oil and gas boreholes</i>	
A.V. Gladilin, S.V. Egerev, O.B. Ovchinnikov	42
<i>Laser ultrasonic technique in diamond anvil cell combined with optical polarimetry</i>	
N. Chigarev, S. Nikitin, A. Zerr, A. Bulou, V. Gusev	43
<i>Photoacoustic spectroscopy based dual channel hygrometer for airborne applications</i>	
D. Tatrai, Z. Bozóki, G. Gulyas, A. Varga, G. Szabó	44
<i>A miniaturized photoacoustic gas sensor fully integrated in Si technology</i>	
J. Rouxel, B. Parvitte, A. Glière, S. Nicoletti, M. Brun, S. Boutami, J. Czarny, A. Walther, R. Vallon, V. Zéninari	45

<i>Application of photoacoustic detection in gas permeation measurements</i>	
N. Tóth, Z. Filus, Z. Bozóki	46
<i>Permeation measurements under extreme conditions using photothermal spectroscopy</i>	
Z. Filus, N. Tóth, Z. Bozóki	47
<i>Applications of photoacoustic resonances for soft matter characterization</i>	
S. Galović, M. Nešić, M. Popović, M.D. Rabasović, D. Markushev	48

APPLICATIONS IN MEDICINE, BIOLOGY AND AGRICULTURE

<i>Study on photoacoustic technique of thermophysical properties of human skin</i>	
A. Yoshida, A. Imuta, T. Yamada, K. Kagata	49
<i>Cavity enhanced absorption spectroscopy and photoacoustic spectroscopy for human breath analysis</i>	
J. Wojtas, F.K. Tittel, T. Stacewicz, Z. Bielecki, R. Lewicki, J. Mikołajczyk, M. Nowakowski, D. Szabra, P. Stefański, J. Tarka	50
<i>Dynamics of thermal denaturation of blood proteins: study with photothermal methods</i>	
E. Sehn, G.V.B. Lukasiewicz, F. Sato, M.L. Baesso	51
<i>Direct estimate of cocoa powder in cakes: colorimetry and photoacoustic approach</i>	
O. Dóka, R. Kulcsár, D. Bicanic	52
<i>Photoacoustic quantification of food colorants in confectionery</i>	
O. Dóka, R. Kulcsár, D. Bicanic, Zs. Ajtony	53
<i>Direct quantification of carotenoids in low fat baby foods via laser photoacoustics and colorimetric index a^*</i>	
O. Dóka, Zs. Ajtony, D. Bicanic, D. Valinger, Gy. Végvári	54
<i>Laser photoacoustic method in dendrochronology: 300-years CO_2 chronology of annual tree rings</i>	
B.G. Ageev, Yu.N. Ponomarev, V.A. Sapozhnikova	55
<i>Investigation on plant pathogen interaction by LPAS sensor</i>	
A. Puiu, G. Giubileo, A. Lai	56

IMAGING

<i>Cluster segmentation of thermal image sequences using kd-tree structure</i>	
R. Świta, Z. Suszyński	58
<i>Photoacoustic signal formation in heterogeneous multi-layered systems with piezoelectric detection</i>	
M.V. Isaiev, D.A. Andrusenko, A.G. Kuzmich, V.V. Lysenko, R. Burbelo	59
<i>Photoacoustic imaging of defects in MEMS</i>	
N. Chigarev, C. Ni, V. Tournat, O. Bou Matar, V. Gusev	60

<i>Advantages and disadvantages of thermal measurements using spatial modulation technique</i>	
M. Kosikowski, Z. Suszyński	61
<i>Photothermal measurements by the use of scanning thermal microscope</i>	
J. Bodzenta, J. Juszczyk, A. Kaźmierczak-Bałata, G. Wielgoszewski	62

ULTRAFAST, MICRO/NANOSCALE AND NONLINEAR PHENOMENA

<i>Nanoscale magnetic characterization by SThM-modulated ferromagnetic resonance</i>	
P. Kijamnajsuk, R. Meckenstock, M. Chirtoc, J. Pelzl	64
<i>Acoustic waves generation in a transparent matrix by host metal nanoparticle illuminated by laser pulses</i>	
N.I. Grigorochuk	65
<i>Photoacoustic discrimination of optical absorbers based on non-linear generation</i>	
A. Prost, O. Simandoux, J. Gâteau, E. Bossy	66

THERMOPHYSICS

<i>Complementary photothermal techniques for complete thermal inspection of solids</i>	
D. Dadarlat, M. Streza, O. Onija, K. Strzałkowski, C. Prejmerean, D. Prodan, L. Silaghi-Dumitrescu, N. Cobirzan	68
<i>Temperature dependence of optical absorption in defect chalcopyrite semiconductor CdGa₂Te₄ studied by photoacoustic spectroscopy</i>	
B.K. Sarkar, A.S. Verma, S. Sharma, P.S. Deviprasadh	69
<i>Photoacoustic elastic bending method: study of the microcantilevers</i>	
D.M. Todorović, D.D. Markushev, M.D. Rabasović, V. Jović, M. Sarajlić	70
<i>Measurement of the thermal parameters of selected II-VI crystals by means of photopyroelectric methods and infrared lock-in thermography</i>	
K. Strzałkowski, D. Dadarlat, M. Streza, A. Marasek	71
<i>Investigation of the influence of rolling on the thermal diffusivity of metal alloys by photothermal infrared radiometry</i>	
I. Delgadillo-Holtfort, B.K. Bein, P. Kijamnajsuk, M. Chirtoc, J. Pelzl	72
<i>Photothermoelastic characterisation of a tuning fork used in infrared and photoacoustic spectroscopy</i>	
M. Spajer, S. Euphrasie, B. Cavalier, X. Vacheret, D. Vernier, G. Matten, P. Vairac, A. Jalocha	73
<i>Photothermal study of the effect of thermal annealing on the thermal interface resistance of Cu-coated carbon and Cu-coated diamond</i>	
N. Horny, J. Hell, M. Chirtoc, P. Kijamnajsuk, C. Eisenmenger-Sittner, J. Pelzl	75

<i>Correlation between the Hall carrier concentration and the effective IR optical absorption coefficient in CdMgSe mixed crystals measured by the photothermal IR-radiometry</i>	
M. Pawlak, M. Maliński, F. Firszt, J. Pelzl, A. Wieck, A. Marasek	76
<i>Modelling of the thermoacoustic frequency characteristics for the air-tightness test method</i>	
M. Kubicki, M. Maliński	77
<i>Investigation of thermal properties of SiC ceramics containing carbon nanostructures by photothermal measurements</i>	
A. Kaźmierczak-Bałata, J. Bodzenta, J. Mazur	78
<i>Analysis of the piezoelectric photothermal spectra of ZnSe, Zn_{1-x-y}Be_yMg_ySe and Zn_{1-x-y}Be_yMn_ySe crystals after different surface treatment</i>	
M. Maliński, J. Zakrzewski, K. Strzałkowski, F. Firszt	78

PREFACE

Intensive development of photoacoustic and photothermal techniques in the past decades has led them no longer being considered just as research topics, but as practical and unique measuring tools. The Conference on Photoacoustic and Photothermal Theory and Applications (CPPTA) has been planned to be a venue where scientists and engineers who deal with photoacoustic or photothermal techniques can share their experiences and ideas. Its scope covers virtually all the aspects of photoacoustic, photothermal and related research, including theory, instrumentation and a wide range of applications:

- theoretical considerations,
- instrumentation and methodology,
- spectroscopy, applications in chemistry,
- sensors, actuators and industrial applications (including environmental sensors, generation of ultrasound, etc.),
- applications in medicine, biology and agriculture,
- imaging (including thermography, tomography, microscopy, depth profiling, etc.),
- ultrafast, micro/nanoscale and nonlinear phenomena,
- thermophysics (including characterization of materials),
- other aspects and applications of PA / PT techniques.

Although it is the first time when the CPPTA is organized, we received quite a lot of submissions. After review of the abstracts, 63 works by over 180 authors were accepted for oral and poster presentations.

We hope that the CPPTA will become a regular event attended by world-top scientists but also available for the young people. Hence, we strongly encourage young researchers to participate in the CPPTA conferences. They will have the opportunity not only to present the results of their research, but most of all, to learn about the latest discoveries and trends, meet the world's experts in the fields of PA / PT, and listen to speeches, during which top international scientists will summarize their experiences and talk about new ideas and perspectives of further development in the PA and PT fields.

Finally, I greatly appreciate very warm reception and a lot of support and valuable advices that I have received from the members of our scientific committee. Their kindness and assistance are difficult to be overestimated.

Tomasz Starecki

(Conference Chair)

KEYNOTE SPEECHES

Photoacoustic spectroscopy in gas sensing and biomedical applications

M.W. Sigrist , J.M. Rey, J. Kottmann

ETH Zürich, Institute for Quantum Electronics, Laboratory for Laser Spectroscopy and Sensing,
Schafmattstrasse 16, CH-8093 Zürich, Switzerland

 sigristm@phys.ethz.ch

The monitoring of trace species is of great interest in various areas ranging from gas sensing to detection of species in liquids, solids and biological materials. Different detection methods have been explored. Best performance with respect to high sensitivity and specificity in multi-component systems is usually achieved with tunable lasers as light sources. However, for moderate sensitivity a (cheaper) LED source may be sufficient. Multi-pass cells, cavity ring-down and photoacoustic detection all offer high sensitivity with the latter usually involving less sophisticated equipment and optical adjustments. Here we illustrate the performance with examples from our own laboratory in gas sensing and glucose monitoring.

The robustness of laser-based photoacoustic gas monitoring has been demonstrated in a field measurement campaign back in 2003 [1]. With a mobile automated CO₂-laser based photoacoustic system implemented in a trailer we have recorded ethylene (C₂H₄), CO₂ and ammonia (NH₃) concentrations consecutively at 5 minute intervals at the exit of a street tunnel by alternating selected wavelengths of a ¹²CO₂ and a ¹³CO₂ laser. The employment of a multi-pass resonant photoacoustic cell equipped with a microphone array allowed the monitoring of ppb concentrations which was by far sufficient for the elevated concentrations measured at this urban site and harsh environment.

More recently, we developed a new photoacoustic concept which permits gas measurements with a simple LED array as light source. The concept is based on the differential mode excitation photoacoustic (DME-PA) technique [2]. This method uses the excitation of two different modes in a resonant photoacoustic cell. The gas concentration is derived from the amplitude ratio of these acoustic modes. With four near-IR LEDs emitting around 1.4 μm with a total power of 3 mW we achieved a ±150 ppmV uncertainty for the measurement of water vapor for a 15 s total acquisition time.

The last example is devoted to glucose measurements in skin samples, a first important step towards *non-invasive* continuous glucose control for diabetes patients. We use a mid-infrared tunable laser source (external cavity quantum cascade laser) emitting around 10 μm wavelength as light source and hence benefit from strong glucose absorption but suffer from strong water absorption, i.e. from a short penetration depth into skin. A special fiber-coupled photoacoustic cell with a volume of only 78 mm³ is placed in direct contact with skin. Epidermal skin samples were brought into contact with aqueous glucose solutions with concentrations of 0.1–10 g/dl. Passive diffusion then results in a variation of the glucose concentration in the skin samples. The time-resolved observation

of glucose diffusion into skin has been achieved in this case with a detection limit of 100 mg/dl (SNR=1), i.e. within the physiological range of 30–500 mg/dl. First promising PA measurements after an oral glucose tolerance test of healthy volunteers and comparison with conventional blood glucose give rise to hope that *non-invasive in vivo* glucose sensing is feasible with this technique.

- [1] D. Marinov, M.W. Sigrist, Photochem. and Photobiol. Sciences **2**, 774–778 (2003)
- [2] J. Rey, C. Romer, M. Gianella, M.W. Sigrist, Appl. Phys. B **100**, 189–194 (2010)
- [3] J. Kottmann, J.M. Rey, J. Luginbühl, E. Reichmann, M.W. Sigrist, Biomed. Opt. Express **3**, 667–680 (2012)

Thermal wave measurements at the nanoscale

J. Pelzl 

Institute of Experimental Physics VI, Ruhr-University, D-44801 Bochum, Germany

 josef.pelzl@rub.de

The local excitation or detection of thermal waves offers a means for spatially resolved non-destructive evaluation of material properties. Beside the thermo-physical parameters which govern the thermal transport also the local variation of optical, magnetic and electrical properties can be explored. Actual research activities try to push the spatial resolution of the photothermal methods towards the nanoscale using scanning thermal near field techniques. The application of a scanning thermal microscope enables photothermal inspection of hot spots and mechanical defects in microelectronic, micro-magnetic and micro-mechanic devices as well as the lateral variation of thermal, optical, mechanical and magnetic properties at the nanoscale.

There are two main schemes to use a scanning near field microscope for nanoscale thermal measurements. The first method relies on the generation of thermal waves by Joule heating of the electronic devices or by resonant absorption electromagnetic radiation such as microwaves in magnetic materials. The detection of the surface temperature oscillations is then effected by a scanning thermal microscope offering lateral resolutions limited only by the lateral extension of the thermal tip as long as the thermal diffusion length is larger than the tip size. Alternatively, the temperature at the tip position can be monitored via the thermal wave induced thermal expansion of the sample surface. The thermo-elastic microscopy offers a higher lateral resolution and also a depth sensitivity. Most importantly, the thermo-elastic response avoids the thermal contact problem inherent to the temperature measurement with a thermal probe in contact with the sample.

The second approach is based on local heating with the tip of a scanning thermal microscope itself. The temperature change induced locally by the nano-heater is detected via temperature sensitive physical property of the sample or is measured indirectly by the probe itself via the temperature induced change of its electrical resistance. The latter is known as 3ω -method and provides a means to measure the thermal conductivity of the sample on the nanoscale.

In this talk some outstanding examples from recent research works will be presented which demonstrate high potentiality of these thermal wave approaches in material science followed by a

discussion of still open questions which are subject of actual fundamental research activities. The examples will comprise the detection and characterization of hot spots in semiconductor devices and spatially resolved infrared and microwave spectroscopy where the thermal probe is applied to measure the heat dissipated during resonance absorption of electromagnetic radiation. Using the 3ω -method the impact of a focused ion-beam treatment on the local thermal conductivity in shape memory alloys could be analyzed and a local calorimetry was established for polymer samples. The part of the lecture devoted to the actual efforts in basic research will address the problem to determine the contact area of the thermal probe on the sample surface and the thermal contact resistance between tip and sample. The knowledge of both quantities forms the basis for a quantitative thermal wave measurement at the nanoscale. Other topics to be discussed comprise the possibility and consequences of quantized thermal transport between tip and sample and the information provided by thermal wave studies of nano-particles. We shall also analyze the possible occurrence of a local spin-Seebeck effect in magnetic materials due to the temperature gradients induced by thermal waves in nano-structured systems.

PLENARY / INVITED TALKS

Photothermal mirror (reflection lens) of glasses and glassy materials

S.E. Bialkowski¹ ✉, G.V.B. Lukasiewicz², N.G.C. Astrath²

¹Department of Chemistry and Biochemistry, Utah State University, Logan, UT 84322-0300
USA

²Departamento de Física, Universidade Estadual de Maringá, Maringá, PR 87020-900, Brazil

✉ stephen.bialkowski@usu.edu

Since the first application of the photothermal mirror to help elucidate the cause of the negative refractive index change in laser heated glasses [1,2] significant progress has been made in understanding the physics of the photothermal mirror produced by both continuous [3] and pulsed laser [4] excitation. The photothermal mirror is formed as a consequence of laser heating of a sample followed by thermal expansion that produces a surface distortion. The divergence of a reflected probe laser beam changes with the time-dependent surface distortion. The analytical signal is detected by monitoring this divergence by using a pinhole placed in far-field of the diverging probe laser beam. The resulting time dependent signal is analyzed using models sensitive to thermal expansion and diffusion coefficients. For samples of known transmittance, the heat capacity and thermal expansion coefficient may also be elucidated.

The talk will first show how modeling using both analytical solutions with semi-infinite boundaries and finite element method (FEM) analysis are used to calculate theoretical signals. The models include both sample and heat coupling fluid layers. FEM solution results are compared to the analytical solutions to determine the degree to which errors in the semi-infinite approximations affect the predicted signals. Sample dimensions are subsequently chosen to allow use of the analytical expressions for experimental data fitting. Because the analytical solutions often involve numerical integration, the data are first smoothed and reduced in size before regression analysis. Regression analysis of data obtained with samples of known thermophysical properties are in good agreement with that expected.


The talk will show the basic thermophysical and measurement theory and discuss the experimental apparatus and associated concerns. Several example applications of this method will be shown which illustrate the utility. Finally, the future prospects for applying this method for rapid material characterization of both solids and fluids will be given. Major problems still exist in the theoretical analysis of solids with rough surfaces, light scattering in transparent and semitransparent materials, and the effects of radiation on the surface of fluids.

[1] O. O. Dada, M. R. Jorgensen, and S. E. Bialkowski, *Appl. Spectr.* **61**, 1373 (2007)


[2] P. R. Joshi, O. O. Dada, and S. E. Bialkowski, *Appl. Spectr.* **63**, 815 (2009)

- [3] L. C. Malacarne, N. G. C. Astrath, G. V. B. Lukasiewicz, E. K. Lenzi, M. L. Baesso, and S. E. Bialkowski, *Appl. Spectr.* **65** 99 (2011)
- [4] G. V. B. Lukasiewicz, N. G. C. Astrath, L. C. Malacarne, L. S. Herculano, V. S. Zanuto, M. L. Baesso, and S. E. Bialkowski, *Appl. Spectr.* (submitted 2013)

High frequency photoacoustic transients generated at surfaces

B. Wu, C. Frez, G.J. Diebold 

Department of Chemistry, Brown University, Providence, 02912 RI, USA

 Gerald_Diebold@Brown.edu

The photoacoustic effect is commonly described by an inhomogeneous wave equation for pressure of the form

$$\left(\nabla^2 - \frac{1}{c^2} \frac{\partial^2}{\partial t^2}\right)p = -\frac{\beta}{c_p} \frac{\partial H(\mathbf{r}, t)}{\partial t} \quad (1)$$

where p is the pressure, c is the sound speed, β is the thermal expansion coefficient, C_p is the specific heat capacity, t is the time, and H is the energy per unit time and volume deposited by the optical source. Equation (1) is derived under the assumption of no heat conduction, which, on physical grounds appears to be a reasonably good assumption, since significant conduction of heat takes place on a time scale that is long compared to sound production. However, in the case of absorbing surfaces in a transparent medium irradiated by a short pulse laser, enormous thermal gradients are generated between the heated surface and surrounding medium which change rapidly in time. Such rapid heat transfer can be expected to produce strong acoustic transients at the leading edge of the photoacoustic wave.

An exact description [1] of the effects of heat diffusion on the photoacoustic effect requires solution of a pair of coupled differential equation, one of which is the heat equation with an additional term accounting for the influence of pressure on temperature. An approximate solution can be found by assuming that the heat capacity ratio is small in the case of liquids so that the coupled equations reduce to

$$\left(\nabla^2 - \frac{1}{c^2} \frac{\partial^2}{\partial t^2}\right)p = -\rho\beta\chi \frac{\partial}{\partial t} \nabla^2 \tau - \frac{\beta}{c_p} \frac{\partial H(\mathbf{r}, t)}{\partial t} \quad (2)$$

where ρ is the density, τ is the temperature, and χ is the thermal diffusivity. Note that the modified wave equation requires a solution to the heat diffusion equation to give τ before the pressure can be determined. Here, the case of a flat, weakly absorbing layer in a one-dimensional geometry irradiated by a laser pulse that is a delta function in time is treated. The solution of the heat diffusion equation presents difficulties as a source in Eq. (2) as it does not obey causality. However, by appropriate approximation, a solution for the pressure can be obtained in closed form that describes a compressive transient on the leading edge of the photoacoustic wave emanating from the irradiated layer.

Experiments were done using the 532 nm, frequency doubled output from a 10 ns Nd:YAG laser to irradiate a soda lime glass target submerged in water. The photoacoustic signal was recorded with a polyvinylidene fluoride thin film transducer. The transducer output was amplified with a high frequency voltage amplifier and fed to an oscilloscope. The target was mounted on precision rotation stages in order to give accurate alignment of the surface of the glass with respect to the surface of the transducer. The signals recorded show a compressive leading edge on the normally square features of the photoacoustic waveform. Slight misalignment of the target by roughly a degree resulted in integration of the transient so that only the square features of the wave remained.

[1] P. M. Morse and K. U. Ingard, *Theoretical Acoustics*, Harwood Academic, Reading, MA (1991)

Laser-based guided ultrasonic bulk (3D), surface (2D), and wedge (1D) waves in (non)destructive evaluation: from macroscopic properties to nanoscopic models

P. Hess¹ , A.M. Lomonosov^{1,2}

¹Institute of Physical Chemistry, University of Heidelberg, D-69120 Heidelberg, Germany

²General Physics Institute, Russian Academy of Sciences, 119991 Moscow, Russian Federation

 peter.hess@urz.uni-heidelberg.de

Current progress in laser ultrasonics employing guided elastic waves is reviewed [1]. Excitation and detection of linear and nonlinear ultrasonic waves by a laser pump-probe setup will be described. This includes ultrasound in three-dimensional (3D) bulk waveguides such as rods or rails, two-dimensional (2D) surface acoustic wave (SAW) pulses, traveling along surfaces and penetrating only about one wavelength deep into the solid, and one-dimensional (1D) wedge waves (WWs), propagating at the apex of a wedge with the elastic energy remaining at the tip of the edge. The emerging field of laser-based excitation and detection of linear and nonlinear WWs and their potential applications will be discussed in detail [2]. The dependence of dispersion and diffraction of ultrasound on the geometry of the system and dimension of wave propagation is considered with respect to the degree of nonlinearity that can be achieved by pulsed laser excitation of elastic waves. Note that with short laser pulses of nanosecond to femtosecond duration a localized desintegration of solids into electrons and ions (plasma) and, as a consequence, efficient formation of steep shocks with gigapascal to terapascal pressure can be achieved by the resulting confined micro-explosions.

Recent applications of linear guided ultrasonic waves (3D to 1D) in nondestructive evaluation (NDE) will be presented. Novel developments in the use of guided bulk waves to monitor flaws in rails, for example, as well as the problems connected with this approach will be discussed. Another important application is the characterization of real partially closed surface-breaking cracks by linear SAW pulses, since failure usually starts at the surface. One-dimensional WWs provide new

possibilities for sensitive evaluation of defects or cracks at the apex of wedges, e.g., in cutting tools or turbine blades. On the other hand, linear WWs recently were also applied in sensor devices and in actuators such as ultrasonic motors or streaming in fluidics.

Strongly nonlinear SAW and WW pulses developing shock fronts during propagation due to nonlinearity could be realized experimentally. Shocked SAW pulses were used to measure the fracture strength of single-crystal silicon for selected crystallographic planes and directions. The measured well-defined critical fracture stresses can be compared directly with *ab initio* calculations if theoretical strengths for these particular configurations are available. With the experimental and theoretical information it is possible to describe the tensile bond-breaking process along the weakest Si{111} cleavage plane on the basis of the Griffith approach. This model introduces a characteristic length scale in the nanometer range. The length scale is identified with the distance between the (111) planes in the ideal crystal lattice in the case of the theoretical strength and the size of the largest defect at the surface in the real crystal, where nucleation of the surface-breaking crack with lowest critical fracture stress takes place. On the basis of the normalized model the defect size can be estimated. The critical fracture stress measured for shock waves propagating along the Si{111} cleavage plane in the <11-2> direction was 4 GPa, while the corresponding theoretical stress for tensile opening of the perfect lattice is 22 GPa. These values point to a defect size of about 9 nm at the surface of the silicon specimen that is responsible for impulsive failure. Thus, this method allows the determination of the effective strength of real materials and the size of the defect responsible for failure. The latter essentially depends on the manufacturing process (“engineering strength”).

[1] P. Hess, A. M. Lomonosov, A. P. Mayer, Ultrasonics (to be published)

[2] A. M. Lomonosov, P. Hess, A. P. Mayer, Appl. Phys. Lett. **101**, 031904-1–4 (2012)

Advances in thermal lens microscopy for detection in microfluidic systems

M. Liu, M. Franko ✉

Laboratory for Environmental Research, University of Nova Gorica,
Vipavska 13, P.O. Box 301, SI-5000 Nova Gorica, Slovenia

✉ mladen.franko@ung.si

Thermal lens microscopy (TLM) [1] as a variation of thermal lens spectrometry (TLS) [2] is one of recent promising developments in photo-thermal spectroscopy towards miniaturization and automation. TLM not only has the advantage of high, but it also offers high temporal (~ ms) and spatial resolution (~ μm). When TLM is coupled to lab-on-chip chemistry these characteristics enable high sample throughput and small volume detection of a variety of compounds with low sample/reagent consumption. In microfluidic chips, which offer a state-of-the-art platform for colorimetric reactions needed to enhance the specificity of TLM detection, the micro-channels provide short diffusion distances and large specific interface areas, contributing to considerable reduction of analysis time compared to conventional chemical analysis.


Due to the very short sample length (below 100 μm), the sensitivity of TLM is still ten to hundred times lower than conventional TLS with 1 cm sample length. Recent investigations in this field have therefore focused on the sensitivity and noise sources in TLM and corresponding optimizations of optical configuration were made for the best signal-to-noise ratio and more sensitive detection in a microfluidic chip. Influence of the flow velocity on the TL signal was analyzed theoretically and experimentally. Optimizations regarding the pump and probe beam parameters (beam waists, offsets, mode mismatching) were made. It was found that an appropriate pump-probe beam offset for certain flow velocity will provide not only a higher sensitivity but also a better response linearity of TLM over three orders of magnitude of concentration. Diffraction limited pump beam excitation is advantageous for space-resolved measurement, while a larger pump beam with ten times lower power density is favorable for higher sensitivity. As a result, a thermal lens microscope constructed in house enabled accurate detection of small changes in absorbance (1.6×10^{-6} AU) in a 50 μm microfluidic channel at 50 mW excitation power.

Despite obvious advantages, TLM was not yet exploited for detection in microfluidic flow injection analysis (μFIA). To demonstrate the advantages and potentials of TLM in μFIA systems, a combined microfluidic-FIA-TLM method was proposed for rapid determination of pollutants by colorimetric reactions. The method was tested by detection of Cr(VI) as a model analyte, following derivatization with diphenylcarbazide, which was previously extensively studied by conventional TLS [3]. It was found that under high excitation power densities (e.g. $> 3 \times 10^4$ W/cm²) the photolabile analytes could be partially degraded, while by increasing the flow rate (e.g. from 20 to 50 $\mu\text{L}/\text{min}$) the degradation of photo-labile analytes can be reduced. Analytical signals for twelve sample injections in one minute have been recorded by the μFIA -TLM. For injections of sub- μL samples into the microfluidic stream in a 50 μm deep micro-channel, limits of detection of 4 ng/mL were achieved for Cr(VI) in water at 60 mW excitation power.

- [1] M. Harada, K. Iwamoto, T. Kitamori, T. Sawada, *Anal. Chem.* **65**, 2938–2940 (1993)
- [2] C. D. Tran, M. Franko, “Thermal Lens Spectroscopy” in: *Encyclopedia of Analytical Chemistry*, ed. R. A. Meyers (John Wiley, Chichester, 2010) DOI: 9780470027318
- [3] A. Madzgalj, M. L. Baesso, M. Franko, *Eur. Phys. J. Special Topics* **153**, 503–506 (2008)

THEORETICAL CONSIDERATIONS

Photodeflection signal formation in photothermal experiments: comparison of existing theoretical description and their application to determination of thermo-optical and structural parameters of TiO₂ based thin films

D. Korte , M. Franko

Laboratory of Environmental Research, University of Nova Gorica,
Vipavska 13, 5000 Nova Gorica, Slovenia

 Dorota.Korte@ung.si

In the photothermal beam deflection technique (PBD) a modulated heating beam illuminates the sample surface. The absorbed energy is converted into heat which diffuses into the sample and gas over it. This induces periodic temperature disturbances that further cause changes in the refractive index of gas close to the sample surface, producing a temporary prism-like optical element. The overall photothermal effect, which depends on thermo-optical properties of the sample and adjacent gas, is detected by a low-power probe beam that is deflected by periodically changing gradient of the gas refractive index.


A couple of theoretical descriptions of this phenomena are known. First of them was introduced by Aamodt and Murphy and is called ray deflection averaging theory (RDAT) [1] in which the PBD signal results from the displacement of the ray in the direction perpendicular to the sample surface. For the probe beam modeled as a bundle of rays the PBD signal is treated as a weighted sum of their contributions. RDAT does not take into account the phase change of the probe beam after its interacting with the field of TL. The second model is called the wave theory (WT) [2] and was proposed by Glazov and Muratkov. According to WT the BD effect is considered to be due solely to phase changes (this is so called the thin lens approximation). This means that only the phase changes in the electric field of the probe beam caused by the probe beam interaction with the thermal wave field are taken into account. Distortions of amplitude distribution caused by deflection on refractive index gradients are not considered.

Lately the analysis of probe beam propagation in thermally disturbed medium is performed on the basis of the complex ray theory (CRT) [3] which allows to take into account disturbance of amplitude and phase of electric field of the probe beam and the probe beam is considered to be a bundle of rays that propagate in a complex space. The probe beam interaction with the field of thermal wave consists of two effects. One is the deflection of the beam and the second is the phase change of the beam. The deflection results from the gradient of the refractive index and causes the ray trajectory change in the temperature field. The ray trajectory change results in the probe beam


amplitude change caused by the change of the divergence of the bundle of rays. The field of thermal wave also influences the beam phase. Its change is caused by the change of the optical path of the ray after propagating through the thermal element (because of the refraction index change) and the change of the geometrical path of the ray (because of the refraction index gradient). In summary, only the CRT takes into account both effects of the probe beam interaction with the field of thermal wave and thus it is expected to provide better description of the analyzed phenomena and thus more reliable determination of thermo-optical parameters of investigated samples. To verify these expectations, a theoretical analysis of PBD signal for various thermal, optical and geometrical parameters of thin films deposited on bulk substrate was performed by the multiparameter fitting of the experimental data to their theoretically predicted values. It was found that the differences between the CRT and RDAT as well as WT can be observed for small values of thermo-optical parameters. The differences in values of thin film's thermo-optical parameters for some chosen samples indicated that thinner the sample is, more pronounced are the differences between all the models.

- [1] L. C. Aamodt, and J. C. Murphy, *J. Appl. Phys.* **52**, 4903–4914 (1981).
- [2] A. L. Glazov, and K. L. Muratkov, *Int. J. Optoelectr.* **4**, 589–597 (1989).
- [3] D. Korte Kobylinska, R. J. Bukowski, B. Burak, J. Bodzenta, S. Kochowski, *J. Appl. Phys.* **100**, 063501-06362 (2006)

Laser-induced wavefront distortion in optical materials

L.C. Malacarne , N.G.C. Astrath

Physics Department, Maringá State University, Maringá, Brazil

 lcmala@dfi.uem.br


Laser induced wavefront distortion in optical components due to thermal lensing and thermally-induced birefringence may affect performance and stability of optical systems, such as high-power lasers, and is also the base of several photothermal techniques. This distortion is a result of complex photoelastic effects that characterize the degradation and the propagation of the beam as a result of a thermal lens by the thermo-optic effect, thermal expansion, and the stress-optic effect. A simple analytical solution for laser-induced beam distortion is well understood and applies only for axially symmetric thermal loadings, with the assumptions that the stresses follow thin-disk or long-rod approximations. In this work [1,2], we developed a generalized theoretical model for the optical path change that is related to the temperature profile in a relatively simple manner for all classes of absorbing optical materials. The modeling is based on the solution of the thermoelastic equation and provides time-dependent expressions for the temperature, surface displacement, and stresses. This generalized model could have a significant impact and provides an analytical tool for designing laser systems. The analytical expressions for optical path change also has direct application in photothermal techniques, which correlate optical path change to thermal, optical, and mechanical properties of solid materials. The theory complements previous work allowing one to access optical distortions of materials ranging from thin-disk to long-rod-like distributions

- [1] L. C. Malacarne, N. G. C. Astrath and M. L. Baesso, J. Opt. Soc. Am. B **29**, 1772-1777 (2012)
[2] L. C. Malacarne, N. G. C. Astrath and L. S. Herculano, J. Opt. Soc. Am. B **29**, 3355-3359 (2012)

Time reversal for PAT in thermo-viscous media based on the wave equation of Nachman, Smith and Waag


R. Kowar 

Department of Mathematics, University of Innsbruck,
Technikerstrasse 21a, 1st floor, A-6020, Innsbruck, Austria

 richard.kowar@uibk.ac.at


This paper is concerned with time reversal for photoacoustic tomography (PAT) of thermo-viscous media based on the wave equation of Nachman, Smith and Waag for one relaxation process. We note that in contrast to the thermo-viscous wave equation, the wave equation of Nachman, Smith and Waag obeys causality, i.e. has a finite wave front speed. Although, in case of dissipative media, the time reversal image $F(\tau, \kappa)$ cannot be the exact initial pressure function φ , we show that $F \rightarrow \varphi$ for the limit $\kappa \rightarrow 0$, where τ and κ denote the relaxation time and compressibility, respectively. Our numerical simulations show that κ is sufficiently small for tissue similar to water such that F is a good approximation of φ . For practical purposes we derive a small wave-number approximation of the time reversal image that permits a comparison with the respective time reversal method based on the thermo-viscous wave equation.

Finite sample size effect in laser induced surface displacement

V.S. Zanuto¹ , L.S. Herculano¹, G.V.B. Lukasiewicz¹, L.C. Malacarne¹, M.L. Baesso¹,
C. Jacinto², N.G.C. Astrath¹

¹Departamento de Física, Universidade Estadual de Maringá, Maringá, PR 87020-900, Brazil

²Instituto de Física, Universidade Federal de Alagoas, Maceió, AL 57072-970, Brazil

 vszanuto@gmail.com

The thermal mirror (TM) method has been widely investigated both theoretically and experimentally over the past few years [1–5]. The thermal mirror technique relies on measuring the time evolution of a laser induced thermoelastic displacement in solid sample. The amplitude of this effect is directly related to the optical absorption coefficient and linear thermal expansion coefficient. In addition, the time evolution depends on the thermal diffusion properties. Monitoring this dynamic


effect allow us to access thermal optical and mechanical properties of the materials. In previous works [1–3], the semi-infinite approximation was employed to solve the heat transfer and thermoelastic equations. This work presents a theoretical and experimental study for the surface deformation for very low optical absorbing materials by taking the finite sample thickness effect into account. The analytical solution for a sample of thickness L is used to model the TM effect and the results are compared with numerical finite element analysis (FEA) solution. The FEA modeling results were found to be in excellent agreement with the analytical solution. In addition to the analytical and FEA analysis, we consider experimental results to validate the finite-size effects on the physical properties of different optical glasses. We show that consistent physical properties could be obtained when sample thickness is taken into account [6,7].

- [1] N. G. C. Astrath, L. C. Malacarne, P. R. B. Pedreira, A. C. Bento, M. L. Baesso, J. Shen, *Appl. Phys. Lett.* **91**, 191908 (2007)
- [2] L. C. Malacarne, F. Sato, P. R. B. Pedreira, A. C. Bento, R. S. Mendes, M. L. Baesso, N. G. C. Astrath, J. Shen, *Appl. Phys. Lett.* **92**, 131903 (2008)
- [3] F. Sato, L. C. Malacarne, P. R. B. Pedreira, M. P. Belancon, R. S. Mendes, M. L. Baesso, N. G. C. Astrath, J. Shen, *J. Appl. Phys.* **104**, 053520 (2008)
- [4] N. G. C. Astrath, F. B. G. Astrath, J. Shen, J. Zhou, C. E. Gu, L. C. Malacarne, P. R. B. Pedreira, A. C. Bneto, M. L. Baesso, *Appl. Phys. B* **94**, 473–481 (2009)
- [5] L. C. Malacarne, N. G. C. Astrath, G. V. B. Lukasiewicz, E. K. Lenzi, M. L. Baesso, S. E. Bialkowski, *Appl. Spec.* **65**, 99–104 (2011)
- [6] N. G. C. Astrath, L. C. Malacarne, V. S. Zanuto, M. P. Belancon, R. S. Mendes, M. L. Baesso, C. Jacinto, *J. Opt. Soc. Am. B* **28**, 1735–1739 (2011)
- [7] V. S. Zanuto, L. S. Herculano, M. L. Baesso, G. V. B. Lukasiewicz, C. Jacinto, L. C. Malacarne, N. G. C. Astrath, *Opt. Mat.* **35**, 1129–1133 (2013)

Single theory of electro-pyroelectric and photo-pyroelectric methods for physical properties investigation

A. Mami , I. Mellouki, N. Yacoubi

U.R. Photopyroelectric, IPEIN, BP 62 Merazka 8000, Nabeul, Tunisia

 mamiamel@gmail.com

In this paper, we proposed a new theoretical model for high accuracy of optical, electrical and thermal parameters of samples measured by two non-destructive Photo-PyroElectric P.P.E. [1] and Electro-PyroElectric E.P.E.[2] techniques.

Instead, pyroelectric response is based on conversion according exciter energy form modulated at frequency f , our approach consisted in uniting theoretical model of two methods in one single theory of pyroelectric signal generating as a function of square root of the modulation frequency, where only heat source term differs. In order to simplify final pyroelectric expression, we are served to normalization procedure relative to alone sensor.

- [1] S. Delenclos, M. Chirtoc, A.H. Sahraoui, C. Kolinsky, J.M. Buisine, Rev. Sci. Instrum. **73**, 2773 (2002)
- [2] N. Bennaji et al, J. Phys. Conf. Ser. **214**, 012138 (2010)

TLM thermal modeling

Z. Suszyński ✉

Koszalin University of Technology, Department of Electronics and Computer Science

✉ zas@man.koszalin.pl

The paper presents a method of modeling of dynamic thermal processes in homogeneous solids, anisotropic ones and layered structures. It uses the idea of the analogy between modeling of 1D heat flow and electromagnetic wave in a waveguide for harmonic excitation. The models can be used for analytical and numerical calculations. To determine the temperature field in discrete analysis the admittance matrix method was used.

Model of the photoacoustic Helmholtz resonator with conical ended duct

M. Suchenek ✉


Institute of Electronic Systems, Warsaw University of Technology,
Nowowiejska 15/19, 00-665 Warsaw, Poland

✉ msu@op.pl

The article presents models of a photoacoustic Helmholtz resonator in which the duct is ended with conical profiles. The analytical descriptions led to poor results and a partly numerical model was presented, in which cone sections of the duct were stepped-approximated by dividing them into number of short segments with different diameters. Accuracy of the model was compared to the best models of photoacoustic Helmholtz cell with the constant diameter duct. Proposed stepped-approximation can be used as well for modeling photoacoustic Helmholtz resonators with other profiles of the duct.

INSTRUMENTATION AND METHODOLOGY


Photoacoustic signal generation in acoustic resonators by periodic trains of laser pulses

A. Miklós¹ , M.G. da Silva², J. Angster³

¹Steinbeis Transfer Centre Applied Acoustics, Landauer Str. 24, D-70499 Stuttgart, Germany

²UENF, Av. Alberto Lamego 2000, Campos dos Goytacazes, RJ, Brasil

³Fraunhofer Institute of Building Physics, Nobelstrasse 12, D-70569 Stuttgart, Germany

 AkustikOptik@t-online.de

Photoacoustic signal is usually generated and detected in a photoacoustic (PA) detector, which contains one or two acoustic resonators, and may contain acoustic buffer and filter elements. The sound signal detected by the microphone is a result of several physical-acoustical processes initiated by the absorption of light energy by the target molecules of the gas mixture that fills the PA detector. It is well known that stationary illumination cannot generate sound; the photoacoustic effect, sound generation by light absorption, can be observed only by modulated or pulsed illumination. In the practice three methods are commonly used; the illumination by an intensity or wavelength modulated continuous wave (cw) laser, the illumination by a single laser pulse and the illumination by a periodic pulse train. PA measurements by single laser pulses have been reported earlier in connection with the application of high-Q acoustic resonators, but this method is only rarely applied recently. PA measurements with periodic pulse trains of different pulsed lasers are quite common and the PA signal generation is described mostly in the literature by the expressions derived for intensity modulated cw lasers. However, the PA signal generation mechanism of a periodic pulse train differs significantly from that of a modulated cw beam. In order to understand the different PA signal generation mechanisms in an acoustic resonator, the three different methods are discussed in details in this paper.

The processes of light absorption by a gas molecule and the following relaxation processes have been investigated by several authors, therefore the presented theoretical considerations are based on the assumption that the excited molecules release the energy of the absorbed light pulse into the gas as a heat pulse localized to the illuminated volume of the gas. This heat pulse then generates a primary sound pulse, which travels back and forth in the acoustic system of the PA detector.


A single pulse will then excite plenty of acoustic eigenresonances of the PA detector. Each eigenresonance responds with a decaying sine signal. The amplitudes and decay rates of the excited eigenmodes may be very different, depending on the detector and beam geometry and the duration of the primary acoustic pulse. It is possible, however, to optimize the PA detector and laser beam for a selected strong eigenresonance. In this case a nice, slowly decaying sine wave may be obtained as PA response for a single pulse excitation.

In the case of periodic pulse trains each pulse excites plenty of resonances. Some of the decaying sine signals will overlap in-phase, thus these components will be amplified. Other components that overlap in opposite phase will be suppressed. If the repetition frequency of the laser pulses is identical with the frequency of an eigenresonance, a strong PA signal may be developed at that frequency. However, the amplitude of the PA signal will depend also on the duration of the primary acoustic pulse, which, in turn, depends on the beam geometry and on other factors, such as the molecular relaxation time. The acoustic excitation of the PA system is usually more effective for higher frequencies in the 10–100 kHz range, while the Q-factor of the eigenresonances decrease with the frequency. These properties allow the optimization of the sensitivity of the PA detector by matching the beam geometry and the repetition rate to the acoustic properties of the PA detector.

Differential open photoacoustic Helmholtz cell

T. Starecki , A. Geras

Institute of Electronic Systems, Warsaw University of Technology,
Nowowiejska 15/19, 00-665 Warsaw, Poland

 t.starecki@ise.pw.edu.pl

There are very few designs of the open photoacoustic Helmholtz cells, and most of them exhibit very strong penetration of the external acoustic noise inside the cell [1-4]. So far the best values of external acoustic noise suppression obtained in such cells was reported at the level of about 50 dB [5]. The paper presents an open photoacoustic Helmholtz cell design with a differential signal detection. Such an approach leads to substantial improvement of the rejection of the signal components resulting from the external acoustic noise.

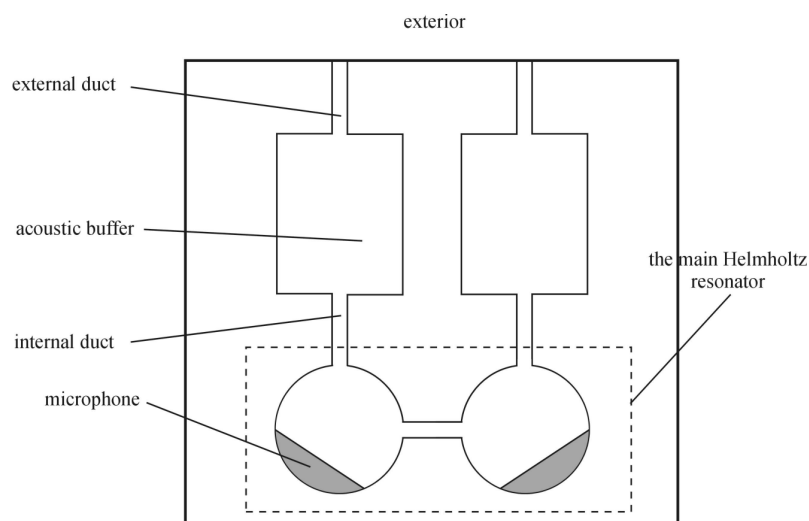


Fig. 1. Structure of the differential open photoacoustic Helmholtz cell.

Structure of the cell is presented in Fig. 1. Both cavities of a conventional Helmholtz resonator (the main Helmholtz resonator) are equipped with microphones and connected with the exterior via duct-buffer-duct structures. Dimensions (length and diameter) of the ducts and volume of the acoustic buffers are selected in such a way that acoustic impedance of the duct-buffer-duct structure at the frequency of light modulation is relatively high. As a result pressure changes induced by the photoacoustic phenomenon inside the cell is not dumped, while penetration of the external acoustic noise inside the cell is limited. Additional rejection of the external acoustic noise signal components is obtained with a differential detection. The cell design is symmetrical in order to obtain nearly identical penetration of the external acoustic noise into both cavities. Hence, subtraction of the signals from both cavities should virtually cancel the external acoustic noise signal components, while doubling the photoacoustic signal component, as in the Helmholtz resonator pressure changes in the cavities are in counterphase.

- [1] T. Diószeghy, A. Miklós, A. Kelemen, A. Lőrincz, *J. Appl. Phys.* **58**, 2105–2109 (1985)
- [2] T. Starecki, *Acta Phys. Pol. A* **114**, A211–215 (2008)
- [3] T. Starecki, *Acta Phys. Pol. A* **114**, A199–204 (2008)
- [4] T. Starecki, A. Geras, *Int. J. Thermophys.*, DOI: 10.1007/s10765-013-1479-y (2013)
- [5] A. Geras, T. Starecki, *Int. J. Thermophys.*, DOI: 10.1007/s10765-013-1497-9 (2013)

Parametric analysis of a differential photoacoustic Helmholtz cell

A. Geras, T. Starecki ✉

Institute of Electronic Systems, Warsaw University of Technology,
Nowowiejska 15/19, 00-665 Warsaw, Poland

✉ t.starecki@ise.pw.edu.pl

The paper describes how mechanical dimensions of a differential open photoacoustic Helmholtz cell [1] affect its operation. Influence of diameter and length of the internal and external ducts and volume of the acoustic buffers on the frequency response of the cell as well as attenuation of the external acoustic noise were studied. The analysis was performed by means of computer simulations based on the loss-improved transmission line model [2]. The results showed that under proper selection of the cell dimensions, its frequency response at the frequencies around the main resonance of the cell is nearly identical as in the case of the conventional, closed Helmholtz resonator. Length of the ducts shows only slight influence on the frequency of resonance, but does not noticeably affect Q-factor of the cell. The results show also that decrease of the duct diameters and increase of the buffers volume improves the attenuation of the external acoustic noise. It should be possible to obtain external acoustic noise rejection as high as 80 dB, which is a substantial improvement in comparison to the previous designs, which reported this value at the level of 40–50 dB [3].

- [1] T. Starecki, A. Geras, presentation „Differential open photoacoustic Helmholtz cell” submitted to CPPTA (2013)
- [2] T. Starecki, *J. Acoust. Soc. Am.* **122**, 2118-2123 (2007)
- [3] A. Geras, T. Starecki, *Int. J. Thermophys.*, DOI: 10.1007/s10765-013-1497-9 (2013)

Improved photoacoustic generator

T. Borowski¹ ✉, M. Suchenek², A. Burd², T. Starecki²

¹independent researcher, Baborowska 5/18, 01-464 Warsaw, Poland

² Institute of Electronic Systems, Warsaw University of Technology,
Nowowiejska 15/19, 00-665 Warsaw, Poland

✉ tomasz.borowski@acn.waw.pl

In conventional photoacoustic experiments photoacoustic signal results from stimulation of the sample with light modulated at a user selected frequency. In the case of photoacoustic generator the output signal is based on self-oscillations resulting from a loop-back in the signal path. Hence, on contrary to conventional photoacoustic methods, frequency of the photoacoustic signal in the photoacoustic generator is self-tuned to the resonance frequency of the photoacoustic cell, which is highly advantageous in the case of high Q-factor resonators.

Previously presented photoacoustic generator designs were producing square wave signals and had a substantial drawback – strongly nonlinear behaviour [1, 2]. The improved version of the generator produces sinusoidal output signal and shows high linearity. Moreover, the automatic gain control signal can be used for determination of the absorption level. The concept of the improved photoacoustic generator was tested in CH₄ concentration measurements.

[1] T.Borowski, T. Starecki, Eur. Phys. J. ST **153**, 439–441 (2008)

[2] T.Borowski, T. Starecki, Eur. Phys. J. ST **154**, 319–323 (2008)

Photoacoustic cell with digital differential detection

M. Suchenek ✉

Institute of Electronic Systems, Warsaw University of Technology,
Nowowiejska 15/19, 00-665 Warsaw, Poland

✉ msu@op.pl

Solutions which reduce impact of the external acoustic noise on the photoacoustic signal rely often on the appropriate modification of the photoacoustic cell structure. The goal is to obtain a frequency response of the cell which suppresses the external noise as much as possible. Another approach is differential detection, in with at least two microphones are used and, assuming that the external noise signal components from both microphones are identical, their subtraction should result in cancelling the external noise. The main difficulty of such a solution is that both microphone signal paths should be calibrated to have virtually identical characteristics. The paper presents differential photoacoustic cell with digital differential detection and software signal calibration. Such a solution is much simpler, as it does not does not require fine tuning of the analog paths of the signal.

A novel method of a photoacoustic cell frequency response evaluation

M. Suchenek ✉

Institute of Electronic Systems, Warsaw University of Technology,
Nowowiejska 15/19, 00-665 Warsaw, Poland

✉ msu@op.pl

The frequency response of a photoacoustic cell can be obtained by measuring the output amplitudes point-by-point at different modulation frequencies, measuring the pulse response or by recording the cell response to a chirp stimulation, in which the light modulation signal is being swept within a given range of frequencies. The paper presents yet another method in which the stimulation signal consists of number of sinusoids with different frequencies. A theoretical description is presented, properties of this techniques are discussed and compared to the experimental results.

Photoacoustic spectroscopy using a MEMS microphone with Inter-IC sound digital output

H. Bruhns, A. Marianovich, M. Wolff ✉

Hamburg University of Applied Sciences, Heinrich Blasius Institute for Physical Technologies,
Berliner Tor 21, D-20099 Hamburg, Germany

✉ marcus.wolff@haw-hamburg.de

In photoacoustic spectroscopy that is adopted for gas sensing, microphones are usually used to detect the pressure variation inside of the sample cell. We present the application of a new commercial I2S digital MEMS microphone that is enhanced with a filter and an analog-to-digital converter in a single package. The utilisation of the described MEMS microphone together with an embedded microcontroller significantly reduces the required space and costs for the components needed to realize the signal detection path of the spectrometer. The measurement results of this signal detection path are compared with those of a conventional photoacoustic spectrometer that is equipped with a capacitive microphone, a microphone preamplifier and a lock-in amplifier for signal processing.

Photoacoustic spectroscopy has become a standard detection method for gases within the last two decades. The sensitivity, resolution, and noise immunity of the generated photoacoustic signal highly depends on the quality of the used microphone and the appropriate signal processing components. Therefore it is always the aim to increase the robustness and quality of the signal detection path of the spectrometers by using new technologies or components. For instance, the quality of the signal detection increased with the application of MEMS microphones instead of capacitive microphones [1]. Although the quality of capacitor microphones also increased, it is still necessary to pre-amplify

the microphone signal and to process it in a lock-in amplifier for the sake of noise reduction, and to convert the analog signal to digital data for processing and documentation. Another step forward can now be made by applying a new generation of digital MEMS microphones consisting of the MEMS microphone, an analog-to-digital converter, a digital filter, a serial port, a hardware control block and a power management block. All these parts fit in a surface mount package of 4.72 mm × 3.76 mm × 1 mm [2]. We placed the digital MEMS microphone together with some other electronic components needed to transform the modulation reference signal of the laser beam on a small printed circuit board. The outputs of the microphone and the reference signal are connected to a microcontroller board for further signal processing. In order to perform a direct comparison between both techniques a special PAS cell was built on which a capacitor microphone and the printed circuit board of the digital MEMS microphone are mounted concurrently. Measurements of the photoacoustic signals of methane as test gas were performed with both microphones in the spectral finger print region.

The digital output of the MEMS microphone is sampled by the microcontroller and transformed to a data format that complies with the regulations for the USB audio device class. Also a USB audio device class stack is implemented in the microcontroller. Therefore, the MEMS microphone's output signal can be recorded with a standard PC audio software tool. The output signal of the condenser microphone is fed in a microphone preamplifier whose output signal is connected to the line input of a USB sound card with 24 bit resolution and recorded with the same PC audio software tool. At the first stage of our study the recorded 24 bit data streams of both microphones are evaluated. At a second stage the digital output signals of the MEMS microphone are processed with the Goertzel algorithm. The results are compared with the digital output of a lock-in amplifier that is connected to the microphone preamplifier's output of the condenser microphone.

- [1] M. Pedersen, J. McClelland, Optimized capacitive MEMS microphone for photoacoustic spectroscopy (PAS) applications, Proc. SPIE 5732, 108 (2005)
- [2] Analog Devices, Omnidirectional Microphone with Bottom Port and I2S Digital Output, ADMP441 Data Sheet Rev. PrG (2011)

Multichannel detection of photoacoustic signals

T. Starecki ¹ ✉, P. Zbysiński²

¹ Institute of Electronic Systems, Warsaw University of Technology,
Nowowiejska 15/19, 00-665 Warsaw, Poland

² BTC Korporacja, Lwowska 5, 05-120 Legionowo, Poland

✉ t.starecki@ise.pw.edu.pl

Use of more than a single microphone (or another pressure sensor) in a photoacoustic instrument is not very common and is limited nearly exclusively to differential setups, in which analog signals from two microphones are subtracted. A solution presented in this paper consists of an array of MEMS microphones. Each of these microphones has dedicated and individually controllable analog

path consisting of a programmable gain amplifier and an A/D converter. Further signal processing is performed in an FPGA circuit. The presented solution allows for placing over ten MEMS microphones on the area comparable to the conventional ½-inch microphone membrane area. As a result it is possible to measure not only an average value of the pressure changes, but also distribution of the pressure field. As such a microphone array can be of virtually any shape (e.g. rectangular), it is possible to adjust it to a particular mechanical design of the photoacoustic cell. Use of multiple microphones increases the overall signal amplitude and allows for signal to noise ratio improvement by means of noise averaging.

SPECTROSCOPY, APPLICATIONS IN CHEMISTRY

Photoacoustic detection of NH₃ by means of a differential double resonator cell

A. Vallespi¹ ✉, V. Slezak¹, A. Peuriot¹, F. González¹, A. Pereyra¹, G. Santiago²

¹CEILAP-CITEDEF San Juan Bautista de La Salle 4397 (B1603ALO) Villa Martelli,
Buenos Aires, Argentina

²Laboratorio Láser, Facultad de Ingeniería, Universidad de Buenos Aires, Paseo Colón 850,
1063 Buenos Aires, Argentina

✉ avallespi@citedef.gob.ar

Ammonia is both a natural and man-made compound. It takes part in countless biological processes and has an increasing relevance in environmental studies. The average global NH₃ concentration in the atmosphere ranges from 0.3 to 6 ppb with sometimes higher values in the environs of agricultural and industrial areas, ranging from 10 ppb to 90 ppb or many orders higher near livestock areas [1]. It is related to acidulation of water sources and eutrophication. Detecting ammonia traces is relevant in health, manufacturing, and security areas, among others. Since ammonia presents a strong absorption band (the ν_2 mode) around 10 μm , we propose its detection by means of photoacoustic spectroscopy (PAS) and study some properties with both a pulsed CO₂ laser (TEA) and a cw CO₂ laser. The laser beam is aimed to an innovative dual resonator differential cell (Fig. 1) designed by means of finite elements method, which lowest resonant frequency is the first longitudinal mode at 1204 Hz. A differential microphone (Knowles NR 23160) is coupled to both resonators [2, 3] at the midpoint of the cell. The characteristics of the differential microphones would minimize noise from distant sources, such as ambient noise and local heating of the cell windows. The chosen cell's material is polypropylene, suitable for reducing the effects of adsorption due to the polarity of the ammonia molecule [4]. In order to take into account error sources during the measurements of low concentrations, physical adsorption-desorption at the cell's walls is studied by means of the record of the PA signal decay using the TEA CO₂ laser. A theoretical model, based on Langmuir's isotherms, fits well the experimental results. As a result, a 5% PA signal decay from an enclosed sample of 248 ppmV of NH₃ in N₂ was registered within 1 hour. Based on this result, minimum errors of the concentrations values are expected from measurements carried out on flowing gas mixtures passing through both resonators. The setup for CW CO₂ laser excitation takes advantage of the differential microphone by picking up out of phase signals. For this purpose, a polished chopper wheel was prepared to allow generating the direct and the reflected beam, alternatively aimed to one resonator and the other. The measurements show that for the double resonator configuration a signal increase is achieved as expected from the study of the sensitivity of both resonators separately, which had been previously characterized. The first measurements with this

system indicate a limit of detection of around 90 ppbV at 1W, defined as the ratio of one standard deviation of PA signal of N_2 to NH_3-N_2 .

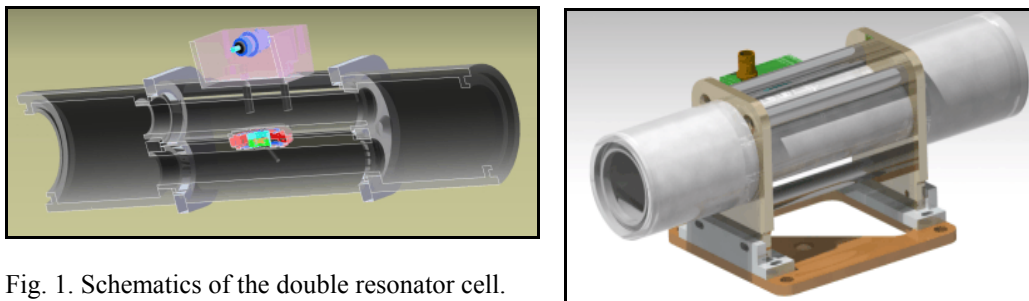



Fig. 1. Schematics of the double resonator cell.

- [1] Agency for Toxic Substances and Disease Registry (ATSDR)
- [2] R. Bernhardt, G. Santiago, V. Slezak, A. Peuriot, M. González. *Sensors and Actuators B* **150**, 513–516 (2010)
- [3] A. Schmohl, A. Miklós, P. Hess., *Appl. Opt.* **41**, (2002)
- [4] N. Melander, J. Henningsen, *AIP Conf. Proc.* **463**, 78–80 (1999)

Single frequency, compact, nested cavity optical parametric oscillators in the 3.3–3.7 μm range: principle and potential for photoacoustic spectroscopy applications

J. Barrientos Barria, J.M. Melkonian, M. Raybaut , J.B. Dherbecourt, A. Godard, M. Lefebvre

Onera, The french aerospace lab, Chemin de la Hunière, F-91761 Palaiseau, France

 myriam.raybaut@onera.fr

For indoor-air quality monitoring, green-house gases monitoring or security applications, there is a need for compact and versatile optical sensors, responding to the demanding specifications for multi-species trace gas detection. For many practical applications, a wide tunability in the 3–3.5 μm wavelength range is interesting since it allows the coverage of strong absorption lines of most green-house or VOC gas species. To be able to detect several species, and address the desired absorption lines without interferences with other species, it is thus required that both the spectral tunability of the

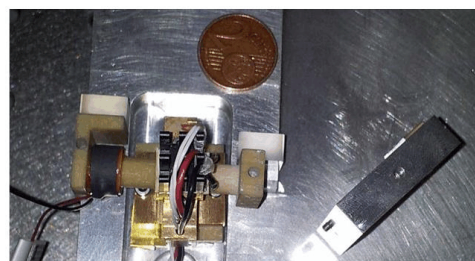


Fig. 1. Compact Nested Cavity OPO architecture, with a 2 eurocent coin for scale.

optical source and the optical bandwidth of the detection scheme be wide. The combination of a single frequency, tunable optical source and a photoacoustic detection scheme could respond to these requirements.

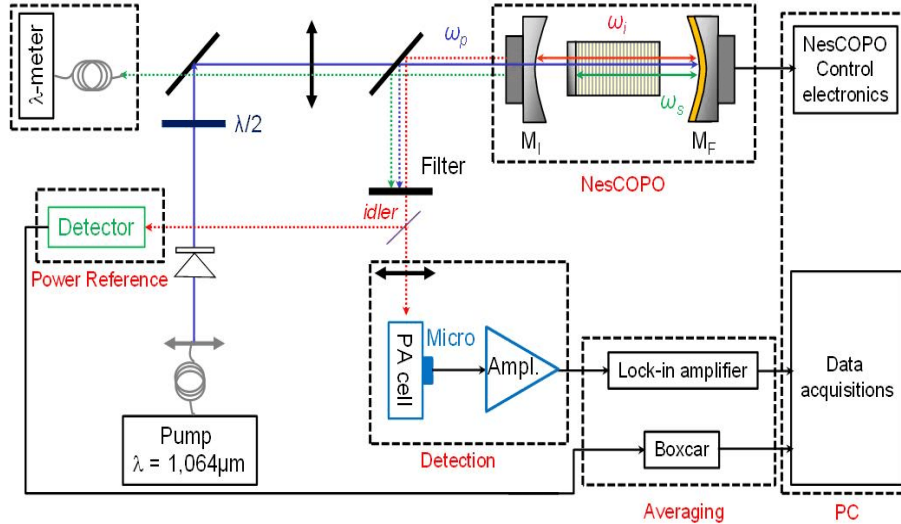


Fig. 2a. Experimental set-up: micro-second, fiber laser pumped NesCOPO, emitting a single frequency radiation in the 3.3-3.7 μm range, coupled to a photoacoustic cell.

Here, we will show that our recent developments in terms of compact (Fig.1), single frequency, pulsed nested cavity optical parametric oscillators (NesCOPO), which can be operated in different temporal regimes, can lead the way to the development of room-temperature, multi-species compact gas sensing systems [1–2].

Performances of a micro-second, fiber laser pumped NesCOPO emitting several tens of mW in the 3.3–3.7 μm range will be detailed. Its potential for photoacoustic spectroscopy will be assessed by coupling of the emitted idler radiation with a non optimized photoacoustic cell, for methane measurement (Fig. 2).

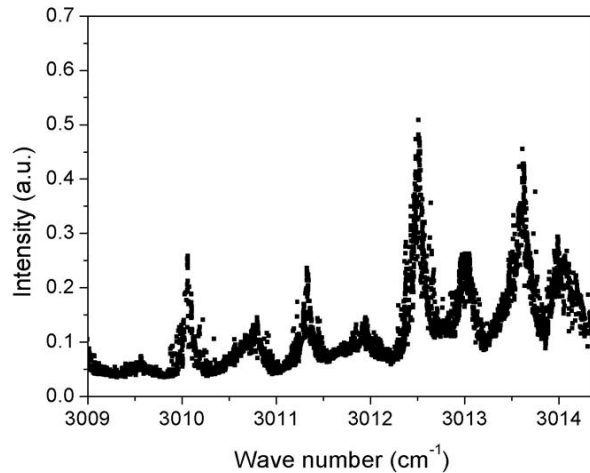



Fig. 2b. Methane and water mixed samples spectrum measurement using this experimental set-up.

- [1] B. Hardy, A. Berrou, S. Guilbaud, M. Raybaut, A. Godard, and M. Lefebvre, *Opt. Lett.* **36**, 678–680 (2011)
- [2] J. Barrientos Barria, J.B. Dherbecourt, M. Raybaut, A. Godard, J.M. Melkonian, and M. Lefebvre, *Europhoton Conference*, Sweden (2012)

Mid-Infrared semiconductor laser based trace gas sensor technologies and applications: state-of-the-art and grand challenges

F.K. Tittel¹ , R. Lewicki^{1,4}, M. Jahjah¹, P. Stefański^{1,3}, J. Tarka^{1,3}, W. Jiang¹, J. Zhang^{1,6}, L. Gong², R. Griffin², S. So⁴, D. Thomazy⁴, P. Lane⁵, R. Talbot⁵

¹Rice University, Electrical & Computer Engineering Department, Houston, TX 77005, USA


²Department of Civil and Environmental Engineering, Rice University, Houston, TX 77005, USA

³Wroclaw University of Technology, Laser & Fiber Electronics Group, Wroclaw, Poland

⁴Sentinel Photonics, Monmouth Junction, NJ 08852, USA

⁵University of Houston, Department of Earth & Atmospheric Sciences, Houston, TX 77204, USA

⁶Northeast Forestry University, Department of Electrochemical Engineering, Harbin, P.R. China

 fkt@rice.edu

This talk will focus on recent advances in the development of sensors based on infrared semiconductor lasers for the detection, quantification and monitoring of trace gas species and their applications in atmospheric chemistry and industrial process control. The development of compact trace gas sensors, in particular based on quantum cascade (QC), interband cascade (IC) lasers, as well as traditional laser diodes permit the targeting of strong fundamental rotational-vibrational transitions in the mid-infrared, that are one to two orders of magnitude more intense than overtone transitions in the near infrared.

The architecture and performance of four sensitive, selective and real-time gas sensor systems based on mid-infrared semiconductor lasers will be described [1]. High detection sensitivity at ppbv and sub-ppbv concentration levels requires sensitivity enhancement schemes such as tunable laser diode absorption spectroscopy (TDLAS) [2, 3] and wavelength modulation spectroscopy (WMS), photo-acoustic absorption spectroscopy (PAS) or quartz-enhanced-PAS (QEPAS) [2-4]. These spectroscopic methods can achieve minimum detectable absorption losses in the range from 10^{-8} to $10^{-11} \text{ cm}^{-1} \text{ Hz}^{-1/2}$.

TDLAS was performed using an ultra-compact, innovative multi-pass gas cell with an effective optical path length of 57.6 m capable of 459 passes between two spherical mirrors separated by 12.5 cm. A 3.36- μm continuous wave (CW) thermoelectrically cooled (TEC), distributed feedback (DFB) GaSb based laser diode operating at 9.5°C was used as the excitation source. For an interference-free C_2H_6 absorption line located at 2976.8 cm^{-1} , a minimum detection limit of 130 pptv with a 1-s acquisition time was achieved. A new state-of-the-art integrated electronic control and data acquisition module was implemented that allowed further significant size reduction without loss of sensor performance.

A QEPAS-based sensor capable of ppbv level detection of CO, a major air pollutant, was developed. We used a 4.61- μm high power CW DFB QCL that emits a maximum optical power of more than 1W in a CW operating mode. For the R6 CO line, located at 2169.2 cm^{-1} , a noise-equivalent sensitivity (NES, 1σ) of 2 ppbv was achieved at atmospheric pressure with a 1-s acquisition time. Furthermore, high performance ($> 100 \text{ mW}$) 5.26 μm and 7.24 μm CW TEC DFB-QCL (mounted in a high heat load (HHL) package)-based QEPAS sensors for atmospheric NO and SO_2 detection will be reported. Minimum detection limits (1σ) of 3 ppb and 100 ppb were achieved for a sampling time of 1 s using interference-free NO and SO_2 absorption lines located at 1900.08 cm^{-1}

and 1380.94 cm^{-1} , respectively [1]. Specific examples include C_2H_6 , NH_3 , NO , CO , SO_2 , CH_4 , and N_2O .

- [1] Rice University Laser Science Group website: <http://ece.rice.edu/lasersci/>
- [2] R. Lewicki, J. Doty, R.F. Curl, F.K. Tittel and G. Wysocki, Proc. of the National Academy of Sciences: 106, 12587-12592 (2009)
- [3] R.F. Curl, F. Capasso, C. Gmachl, A. A. Kosterev, J. B. McManus, R. Lewicki, M. Pusharsky, G. Wysocki, F.K. Tittel, Chem. Phys. Lett., 487, 1 (2010)
- [4] L. Dong, A.A. Kosterev, D. Thomazy, F.K. Tittel, Appl. Phys. B 100, 627–635 (2010)

Determination of the singlet oxygen generation efficiency of dyes by applying absorption and optoacoustic spectroscopies

M. Kotkowiak¹ ✉, E. Robak^{1,2}, A. Dudkowiak¹

¹Faculty of Technical Physics, Poznan University of Technology, Nieszawska 13A,
60-965 Poznań, Poland

²Nanobiomedical Centre, Umultowska 85, 61-614 Poznań, Poland

✉ michal.kotkowiak@doctorate.put.poznan.pl

Photodynamic therapy (PDT) has recently become widely used in clinical treatment of different types of diseases. In PDT, absorption of light by a dye leads to generation of an reactive forms of oxygen. Mechanism of PDT involves two types of reactions – direct interaction of the sensitizer in the triplet state with cell tissues (photochemical reaction) – I type reaction and production of the singlet oxygen ($^1\text{O}_2$) – II type reaction [1]. One of the most important features characterizing dye-photosensitizer is the singlet oxygen quantum yield (ϕ_A). The ϕ_A value is a quantitative parameter which describes the ability of photosensitizers to convert and transfer absorbed energy to molecular oxygen to form the singlet oxygen, $\text{O}_2(^1\Delta_g)$, acting as a cytotoxic species.

This study was focused on comparing of two independent methods for ϕ_A determination of photoactive dye molecules. The first method was the time resolved laser-induced optoacoustics spectroscopy (LIOAS). It provides information on the non-radiative fast deactivation of excited singlet states and depopulation of the long-lived states of the dye. Finally, depending on experimental conditions, the analysis of LIOAS signal permits estimation of the yield of dye triplet formation and reactive oxygen species generation [1]. The second method of ϕ_A estimation is based on the photooxidation reaction of 1,3-diphenylisobenzofuran (DPBF) well-known as $^1\text{O}_2$ trap [3]. The dye irradiated with light of a specific wavelength interacts with molecular oxygen, which leads to generation of singlet oxygen. As a result of interaction with $^1\text{O}_2$, DPBF decomposes to 1,2-dibenzoylbenzene which results in a decrease in absorbance (at 417 nm).

For both methods, the choice of reference dyes is crucial, therefore a comparison of independently obtained results was made. The results presented show that the methods allow a reliable

determination of ϕ_A parameter of the dye studied and confirm the correctness of the applied procedure of ϕ_A evaluation.


This work was supported by the Poznan University of Technology (DS 62-213/13).

- [1] M. C. DeRosa, R. J. Crutchley, *Coordination Chemistry Reviews* **233**, 351–371 (2002)
- [2] B. Olejarz, B. Bursa, I. Szyperka, R.-M. Ion, A. Dudkowiak, *Int. J. Thermophys.* **31**, 163–171 (2010)
- [3] J. Piskorz, P. Skupin, S. Lijewski, M. Korpusiński, M. Sciepura, K. Konopka, T. Goliński, J. Mielcarek, *J. Fluorine Chem.* **135**, 265–271 (2012)

Wavelength dependent optical absorption of atmospheric aerosol measured by multi-wavelength photoacoustic spectrometer: a laboratory and a field study

N. Utry, T. Ajtai , Á. Filep, Z. Bozóki, G. Szabó

Department of Optics and Quantum Electronics, University of Szeged, Hungary

 ajtai@physx.u-szeged.hu

One of the largest uncertainties in global radiative forcing calculations associates to carbon content of ambient bulk, therefore the atmospheric aerosol absorption measurements are at the central interest in climate research today. Very recently, multi-wavelength PA instruments become available [1, 2] and open up a novel perspective on direct, real-time investigation of ambient carbon content. In this study we present first, mass specific light absorption coefficient of climate relevant dust compositions such as illit, cao-linite, quartz, muscovite hematite and HULIS aerosol in the whole climate essential and the photochemically active UV region. The measurements were made by our state-of-the-art multi-wavelength photoacoustic instrument (4λ -PAS). We

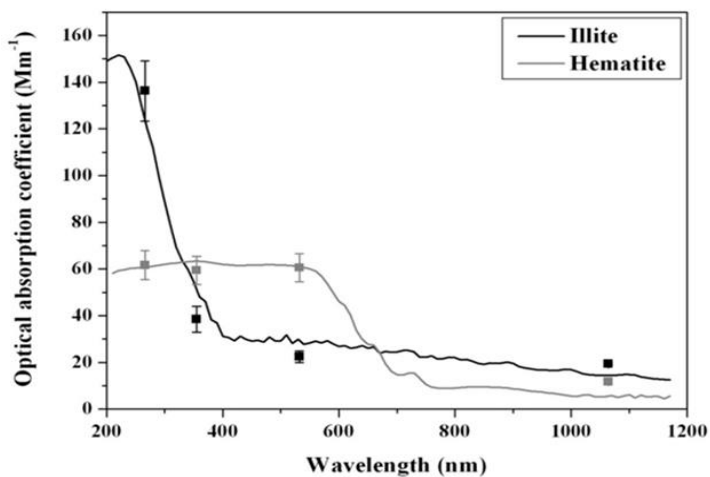


Fig. 1. The photoacoustically measured optical absorption of illite and hematite particles (squares) and its theoretical verification using Mie-model calculations (solid lines).

introduce here a wavelength range specific AAE as a chemically selective parameter. We also present here results of in-situ spectral responses of ambient under winter condition. The hourly concentration of other aerosol variables such as gaseous pollutants (CO and NO_x), trace elements (i.e. K, Ca, Fe, and Si) as well as the size distribution of ambient were also analyzed. The levoglucosan measurement was made to confirm that the daily fluctuation of ambient AAE is driven mainly by the changes in the relative strength between the traffic and residential heating emission. Finally, we demonstrate correlation between the segregated AAEs and other aerosol variables. In all correlation the single and wavelength dependent AAE approach are compared.

Financial support by the Hungarian Scientific Research Foundation (OTKA, Grant no. K101905) is gratefully acknowledged. The European Union and the European Social Fund have provided financial support to the project under the grant no. TÁMOP 4.2.2.A-11/1/KONV.

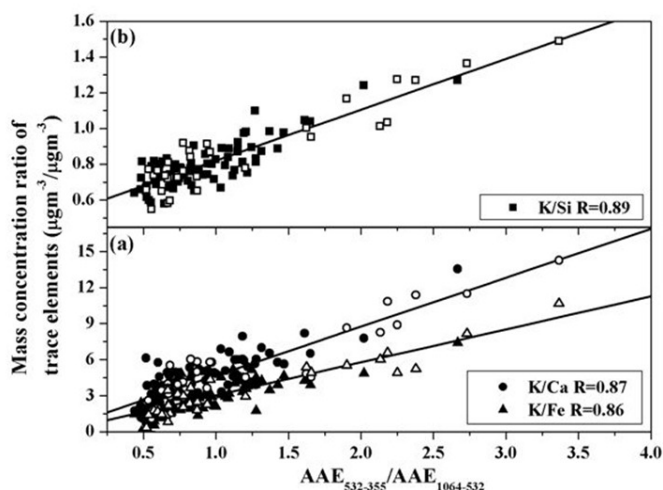


Fig. 2. The correlation between the mass concentration ratio of different trace elements and the ratio of AAE measured photoacoustically at different wavelength range.

- [1] T. Ajtai, Á. Filep, M. Schnaiter, C. Linke, M. Vragel, Z. Bozóki, G. Szabó, T. Leisner, *J. Aer. Sci.* **41**, 1020–1029, (2010)
- [2] K. Lewis, W. P. Arnott, H. Moosmüller, C. E. Wold, *J. Geophys. Res.* **113**, D16203, DOI:10.1029/2007JD009699 (2008)

Dual channel diode laser spectrometer with ring type photoacoustic detector for high resolution spectroscopy and gas analysis

Yu.N. Ponomarev , V.A. Kapitanov

V.E. Zuev Institute of Atmospheric Optics SB RAS
Acad. Zuev Square 1, 634021 Tomsk, Russian Federation

yupon@iao.ru

We present results of the development of photoacoustic spectrometers (PAS) with tunable diode lasers. A two channel PAS with a photoacoustic detector in the form of a ring type (Helmholtz)

resonator provides threshold sensitivity $2 \cdot 10^{-9} \text{ cm}^{-1} \text{ Hz}^{-1/2} \text{ W}$ when the signal to noise ratio equals 1. A Tec-100 diode laser with an outer resonator generates a continuous single-frequency radiation within $6030 - 6300 \text{ cm}^{-1}$ spectral range. We demonstrate applications of this PA TDLS to study of high-resolution absorption spectrum of CH_4 near $1,65$ ($2\nu_3$ band) and study the broadening and shifting of the overlapping spectral lines induced by collisions with noble atoms and molecules with uncertainty less than 2% for absorption cross-sections, broadening and shift coefficients [1, 2]. To improve PAS characteristics (S/N ratio, sensitivity) we designed a high quality mirror chopper. The results of its testing are discussed. The application of PAS with $1,65 \mu\text{m}$ diode laser applied to monitoring of CH_4 emission kinetics from coal samples and biological systems is demonstrated.


This work is particularly supported by project VIII.80.1.1 SB RAS.

- [1] V.A. Kapitanov, K.Yu. Osipov, A.E. Protasevich, Yu.N. Ponomarev, *JQSRT*, **113**, 1985–1992 (2012)
- [2] K.Yu. Osipov, A.E. Protasevich, V.A. Kapitanov, Ya.Ya Ponurovskii, *Appl.Phys. B*, **106**, 725–732 (2012)

Investigation of the photobleaching process of eosin Y in aqueous solution by thermal lens spectroscopy

L.S. Herculano, L.C. Malacarne, N.G.C. Astrath 


Departamento de Física, Universidade Estadual de Maringá,
Av. Colombo 5790, Maringá - PR, 87020-900, Brazil

 astrathngc@pq.cnpq.br


Eosin Y is known to be a powerful probe of biological molecules and an efficient photosensitizing agent for the production of singlet molecular oxygen. Under continuous laser excitation, degradation through photobleaching is observed in aqueous solutions of eosin Y; this process is driven by the production of singlet oxygen. Optical bleaching in aqueous solutions is known to yield anomalous thermal lens transient signals, which can be evaluated by modeling the relaxation processes that give rise to the generation of heat in the solution. In this work, we investigate the temperature-dependence of molecular diffusion and the kinetics of the reactions of aqueous solutions of eosin Y using time-resolved thermal lens spectroscopy. The results show that the photobleaching of eosin Y has a significant effect on the thermal lens signal. Considering the reaction kinetics and molecular diffusion, we have modeled the optical bleaching. Molecular diffusion drives the photochemically modified species to a steady state, and the transient signal changes accordingly. Using this model, quantitative information regarding molecular diffusion rate, optical bleaching and fluorescence quantum efficiency is obtained. The temperature dependences of the physical parameters were found to be in agreement with literature data for organic dyes. Although the model was developed specifically for a first-order or pseudo first-order relaxation process, it should be suitable for describing more complex systems. The results presented here demonstrate that time-resolved thermal lens

spectroscopy can be used as a very sensitive analytical tool for quantitative measurement of relaxation processes in aqueous solutions.

Photoacoustic spectroscopy of improvised explosive device precursors

A. Puiu , G. Giubileo, A. Palucci

ENEA Frascati, Via E. Fermi 45, 00044 Rome, Italy

 adriana.puiu@enea.it

Explosives in the hands of terrorists continue to pose a significant threat. The most prevalent form of explosive device utilized by terrorists today is the Improvised Explosive Device (IED). IEDs are homemade, non-conventional explosives, fabricated by combining common chemicals. When traditional explosives become difficult to obtain, bomb makers turn to chemicals commercially available in hardware stores, pharmacies and cosmetics stores, as precursors to manufacture explosives. The number of explosives which can be quite easily home-manufactured, is only limited by the imagination and the availability of certain non specific chemicals.

We approached the fight to the increased realization of modern bombs for criminal use, by developing a fast real-time easy-to-use method for the detection of IED precursors based on Infrared Photo-acoustic Spectroscopy (IR-LPAS). IR-LPAS already demonstrated to be promising in the design of an integrated optical system for the real time detection and identification of explosive species in traces to support homeland security.


In this paper we report the LPAS analysis of a number of common chemicals used as IED precursors: potassium sulfate, potassium nitrate, magnesium sulfate, ammonium perchlorate, ammonium nitrate, and acetone. The analyzed chemical species were classified by PCA statistics, applied to the collected spectral data, which facilitate the recognition capability of the adopted method.

SENSORS, ACTUATORS AND INDUSTRIAL APPLICATIONS

Sensing mechanical properties of rocks and sediments by means of optoacoustics while drilling oil and gas boreholes

A.V. Gladilin, S.V. Egerev , O.B. Ovchinnikov

Andreyev Acoustics Institute
4 Shvernika street, Moscow 117036, Russia

 segerev@gmail.com

The paper deals with industrial applications of laser-generated ultrasound, namely with optoacoustical (OA) sensing mechanical properties of rocks and sediments while drilling oil and gas boreholes. A brief review of achievements in the field is given. OA sensing of seismic anisotropy is considered in details.

Seismic anisotropy plays an important role in the exploration of subsurface oil and gas reservoirs. The anisotropy parameters are used not only to improve imaging of the reservoirs but also for more accurate interpretation of seismic data and processing results. Because of this need, there is a demand in the oil and gas industry to obtain anisotropy information from borehole measurements. Anisotropy parameters governing the compressional wave (P-wave) propagation are of primary interest. Determining the P-wave related anisotropy parameters has thus become an important challenge for the borehole acoustic measurements. P-wave anisotropy is manifested by a change in the compressional wave velocity with direction of propagation in earth formations due to combined effects of sedimentary layering and the intrinsic anisotropy of the rock. Shales, in particular, could exhibit more than a 20% difference in P-wave velocities parallel to bedding and P-wave velocities perpendicular to bedding.

For a vertical borehole, the traditional acoustic logging based on analysis of the head wave gives the vertical P-wave velocity component. For a horizontal borehole, the traditional acoustic logging will give the horizontal P-wave velocity component. It is highly desirable to have a localized method of determination of seismic velocities as a function of angle of propagation in an earth formation using high-quality borehole measurements.

OA sensing is based on the laser sound generation by irradiating a spot on the wall of a borehole. The trace of the outgoing bulk sound P-wave pulse propagating along the borehole surface has a velocity depending on its direction. We provide simultaneous measurements of the pulse propagation time along two orthogonal paths. This helps to derive anisotropy parameters of the rock sample. The advantage of a laser generated sound source is its precise positioning on the wall as well as good accuracy of evaluation of the pulse propagation time along the given path. In the paper, waveform of an outgoing laser induced pulse as well as propagation peculiarities are described. Experimental modeling was fulfilled this test being aimed to support accurate depth imaging of seismic data.

- [1] L. Thomsen, *Geophysics* **51**, 1954–1966 (1986)
- [2] X. Tang, Y. Zheng, D. Patterson, *Method for processing reflections in array data to image near-borehole geological structure* (US Patent application 584–42216, 2005)
- [3] A.A. Karabutov, V.A. Makarov, E.B. Cherepetskaya, V.L. Shkuratnik, *Laser-ultrasound spectroscopy of rocks* (Moscow, Gornaya Kniga Publishers, 2008, in Russian)
- [4] D.A. Hutchins, R.J. Dewhurst, S.B. Palmer, *Journ. Acoust. Soc. Amer.* **70**, 1362–1369 (1981)
- [5] L.R. Rose, *Journ. Acoust. Soc. Amer.* **75**, 723–732 (1984)
- [6] T.W. Murray, J.W. Wagner, *J. Appl. Phys.* **85**, 2031–2040 (1999)
- [7] C.M. Scala, P.A. Doyle, *Journ. Acoust. Soc. Amer.* **85**, 1569–1576 (1989)

Laser ultrasonic technique in diamond anvil cell combined with optical polarimetry

N. Chigarev¹ , S. Nikitin^{1,2,3}, A. Zerr², A. Bulou³, V. Gusev³

¹LAUM, UMR-CNRS 6613, Université du Maine, Le Mans, France

²LSPM, UPR-CNRS 3407, Université Paris Nord, Villetaneuse, France

³IMMM, UMR-CNRS 6283, Université du Maine, Le Mans, France

nikolay.chigarev@univ-lemans.fr

Laser ultrasonic (LU) technique [1, 2] provides excellent opportunities for the evaluation of elastic properties of materials in diamond anvil cell (DAC). This LUDAC technique has been successfully applied for the measurement of longitudinal and shear sound velocities of iron up to the pressure of 23 GPa. Recently, it has been shown that significant improvement in the detection sensitivity of shear acoustic waves in LU experiments could be obtained by the introduction of transient optical polarimetry [3] scheme. In this work, we optimise the optical polarimetry to improve the sensitivity of the LUDAC technique to the detection of shear waves at high pressures.

Several modifications, allowing the control of the polarisation of incident and reflected probe laser beam, have been introduced in the experimental set-up [1, 2]. The acoustic pulse, arriving on the interface between the iron film and diamond, induces small transient changes of the polarisation of the reflected probe beam. The polarisation of reflected beam is controlled by the polarizer to convert the change in the polarisation into the change of power on the photo-detector. The optimisation of sensitivity to the detection of shear waves, propagating in the film, is achieved by the

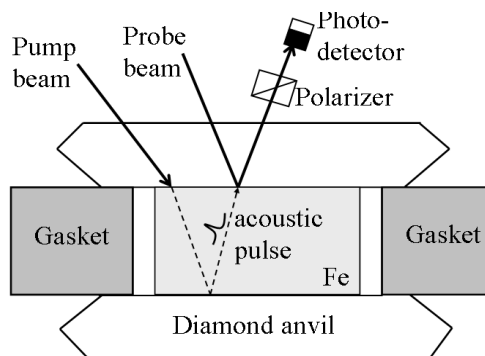


Fig. 1. Configuration of Laser Ultrasonic technique combined with optical polarimetry .

proper choice of the incident polarisation and the angle of the incidence of the probe light. The theory [3,4] is used to guide the optimization in the detection of shear acoustic echoes.

This research is supported by the grant ANR-LUDACism.


- [1] N. Chigarev et al., Appl. Phys. Lett. **93**, 181905 (2008)
- [2] N. Chigarev, P. Zinin, D. Mounier, A. Bulou, A. Zerr, L. C. Ming, V. Gusev, J. Phys.: Conf. Ser. **278**, 012017 (2011)
- [3] D. Mounier, E. Morozov, P. Ruello, M. Edely, P. Babilotte, C. Mechri, J.-M. Breteau, V. Gusev, J. Phys.: Conf. Ser. **92**, 012179 (2007)
- [4] D. Mounier, P. Picart, P. Babilotte, P. Ruello, J.-M. Breteau, T. Pézeril, G. Vaudel, M. Kouyaté, V. Gusev, Opt. Expr. **18**, 6767 (2010)

Photoacoustic spectroscopy based dual channel hygrometer for airborne applications

D. Tatrai¹ , Z. Bozóki^{1,2}, G. Gulyas², A. Varga², G. Szabó¹

¹University of Szeged

²Hilase Ltd.

 tatraid@titan.physx.u-szeged.hu


The importance of accurately measuring humidity (water vapor and total water content) with high space-time resolution for meteorology or climate research is evidence. For humidity measurements several balloon borne or airborne instruments are available. Many of the commercially available ones have quite long response time and are suffering from overshooting effects, that's why many research institutes have developed their TDL or Lyman-alpha spectroscopy based special purpose instruments. But these due to their operational principle these are limited in dynamic range and are only one channel ones so proper only for water vapor concentration or for total water content measurements. At University of Szeged in cooperation with Hilase Ltd a tunable diode laser based dual channel photoacoustic spectroscopy based hygrometer with real time concentration calculation option has been developed. Besides six orders of magnitude dynamic range and subppm detection limit the main advantage of this instrument is that it can measure humidity simultaneously from two independent sources. In case of using proper sampling system this feature gives the possibility for simultaneous water vapor concentration and total water content measurement. One prototype of this instrument has been operated in the CARIBIC project for many years and one in the EUFAR/DENCHAR project.

The measurement system is based on a programmable DSP based electronics, a fiber coupled DFB diode laser at 1392 nm, two single longitudinal mode differential photoacoustic cells, two pressure sensors and gas handling system. This simple but robust layout and the effective noise cancelling of the photoacoustic cells makes the system proper for airborne applications.

The wavelength of the laser is stabilized by its temperature and accurately set by current tuning with at least 50fm accuracy. The possible wavelength drifts due to ageing and external effects are


measured and automatically compensated. The pressure dependent line broadening and shifting of the water vapor absorption line are taken into account during both the calibration and data evaluation. The instrument has been successfully tested during both blind laboratory and flight comparisons. The layout and detailed performance of the instrument will be presented.

A miniaturized photoacoustic gas sensor fully integrated in Si technology

J. Rouxel^{1,2} , B. Parvitte¹, A. Glière², S. Nicoletti², M. Brun², S. Boutami²,
J. Czarny², A. Walther², R. Vallon¹, V. Zéninari¹

¹Groupe de Spectrométrie Moléculaire et Atmosphérique, UMR 7331 CNRS - Université de Reims, Faculté des Sciences, Moulin de la Housse, BP 1039, 51687 Reims Cedex 2, France

²CEA, LETI, MINATEC, 17, rue des Martyrs, F-38054 Grenoble, France

 justin.rouxel@cea.fr

Gas sensor technology based on optical detection has already proven to be crucial for various aspects in our modern society (chemical emission monitoring, process control, high sensitivity trace detection). However, available optical gas sensors are bulky, complex and have a very high cost of ownership. The consequence is that they are not suitable for mass deployment, for instance in sensor networks. Among possible improvements, miniaturization of the gas sensor and associated cost reduction are of primary importance in many application areas with very high socio-economic implications, such as climate change assessment and air quality control.

Photoacoustic (PA) detection is a powerful technique for gas detection at trace level based on optical absorption and subsequent thermal perturbation of the gases [1]. The realization of a miniaturized and integrated photoacoustic cell (μ -PA) would be of great interest to expand the use of such sensors because the detection characteristics scale favourably when the system dimensions are decreased. Furthermore, using Si technologies enables to benefit from the massively parallel integration capabilities of IC and MEMS procedures. However, several technical bottlenecks must be overcome, mainly regarding the integration of laser source, photonic integrated circuit and MEMS microphones. In this concern, it has been shown that detection in the MIR range can be made efficiently with Quantum Cascade Lasers (QCL) coupled with MIR waveguides [2] and MIR waveguides compatible with CMOS technologies have been presented [3]. Moreover, MEMS microphones are now widely available, as demonstrated by their use in smartphones. These achievements open the way for a full integration of a μ -PA module on a single chip. In order to optimize the cost of development of such sensors, their response must be accurately predicted by modelling and simulation during the design stage. Macroscopic PA cells have been successfully simulated [4] but miniaturization and integration involve modelling challenges as, for instance, thermal and viscous surface losses are no longer negligible. Specific models must be devised to meet these original requirements [5].

A first design of μ -PA cell is presented in the full paper. Using the Finite Element Method based model, which takes into account thermo-viscous acoustic effects, the signal and frequency behaviour of the miniaturized and integrated PA sensor is analysed. Finally, compatibility with IC and MEMS procedures and technologies are discussed.

- [1] M. W. Sigrist, *Air Monitoring by Spectroscopic Techniques* (John Wiley & Sons, 1994)
- [2] M. Carras, M. Garcia, X. Marcadet, O. Parillaud A. De Rossi, S. Bansropun, *Appl. Phys. Lett.* **93**, 011109, 2008
- [3] M. Carras, G. Maison, V. Trinité, B. Simozrag, M. Brun, P. Labeye, S. Nicoletti, *Photonics West, OPTO*, 8631-34, 2013
- [4] B. Parvitte, C. Risser, R. Vallon, et V. Zéninari, *Appl. Phys. B*, online March 2013
- [5] A. Glière, J. Rouxel, B. Parvitte, S. Boutami, V. Zéninari, manuscript in preparation

Application of photoacoustic detection in gas permeation measurements

N. Tóth¹ , Z. Filus², Z. Bozóki¹

¹Department of Optics and Quantum Electronics, University of Szeged,
6720 Szeged Dóm tér 9., Hungary

²Permeation Testing Laboratory of Hilase Development, Production, Service and Trading Limited
Company. 6727 Szeged, Irinyi J. u. 1, Hungary

tnikolett@titan.physx.u-szeged.hu

Outstanding features of laser photoacoustic (PA) detection like high sensitivity, excellent selectivity, exceptional reliability, possibility of online monitoring and fully automatic operation make photoacoustics an optimal method in various gas monitoring applications. One of the very promising

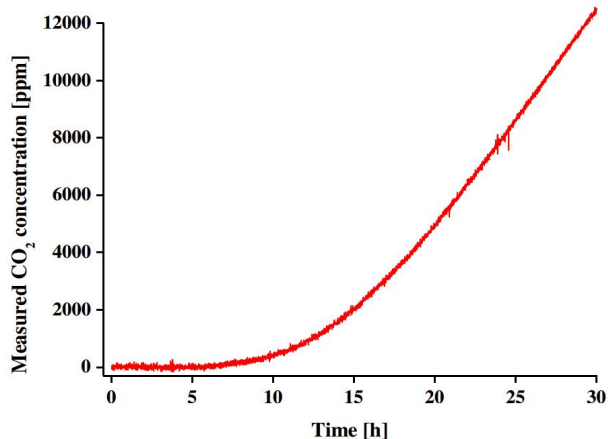


Fig. 1. CO₂ permeability of polymer sample at room temperature

applications of the PA method is permeation testing, i.e. detecting the permeation of analyte molecules through polymer membranes by using a properly optimized configuration of a PA system. A permeation testing set-up consists of a PA detection unit (which is built from a laser light source, a PA cell and an electronic system) and a diffusion cell with two compartments (i.e. source and receiving chambers) separated hermetically by the membrane placed in-between them. The advantages of such combination compared to conventional permeation testing methods are the in-situ analysis without any need of sampling, possibility of

easy configuration modifications and fully automatic operation controlled by a single electronic system. The wide dynamic range of PA method makes this application a unique possibility for measuring and evaluating the whole permeation process without any need of detector replacement or adjustment. The authors developed and successfully tested various versions of a PA detection

based permeation testing system. In the first version the permeated analyte is transferred into the PA cell by a carrier gas flow, in the second version the carrier flow is circulated in a closed loop between the PA cell and the diffusion cell and in the third version the PA cell is built into the receiving chamber of the diffusion cell. As permeation processes can occur on varied time scales the selection of the proper measuring set-up is crucial. A fast permeation process can be completed in seconds and correspondingly the testing system must have short response time, while for barrier samples with extremely low permeability permeation tests can last for several weeks and the testing system has to have extremely high stability. For the different processes different versions of the PA detection based permeation system can be used. Figure 1 shows one example of the measurement demonstrating the excellent signal to noise ratio of the measurements. Different analytes such as methane, ammonia, water vapor, hydrogen-sulfide etc. were measured as well.

Permeation measurements under extreme conditions using photothermal spectroscopy

Z. Filus¹ ✉, N. Tóth², Z. Bozóki²

¹Permeation Testing Laboratory of Hilase Development, Production, Service and Trading Limited. 6727 Szeged, Irinyi J. u. 1. Hungary

² Department of Optics and Quantum Electronics, University of Szeged, 6720 Szeged Dóm tér 9, Hungary

✉ zoltan.filus@hilase.hu

Photothermal beam deflection (PDB) is an optimum tool in gas monitoring systems where high sensitivity, selectivity and wide dynamic ranges are required with a combination of experimental conditions where no sampling can be carried out. In our presentation PBD technique used in collinear arrangement for methane, carbon-dioxide and hydrogen-sulphide diffusion measurements through rubber and polymers sheets will be presented. The presented method enables to perform permeation tests at high pressures (up to 500 bar) and at high temperatures (up to 130°C) too where the detection had to occur in-situ in a closed chamber without contacting or opening it to avoid disturbing the permeation process. Diffusion cell is the main part of permeability measurements with two chambers (feeding and receiving) hermetically separated by the measured polymer sample. The optical windows made from sapphire with specially designed gaskets make the receiving chamber accessible by the lasers beams. The permeation process is initiated by filling the source and receiving chambers with high pressure methane and nitrogen gases, respectively. The equality of the pressures is controlled very accurately in the chambers during the filling process in order to avoid damage of the sample sheet. Driving force of the diffusion process is the partial pressure i.e. concentration difference of analyte, therefore, it is possible to record the concentration of the permeated molecules in the receiving chamber. Permeation parameters are calculated from the diffusion curve, i.e. the concentration of the analyte as a function of time.

The pump laser for photothermal signal generation was a DFB diode laser amplitude modulated at 70 Hz being partially absorbed by the measured molecules, while the probe laser was a 660 nm

DFB diode laser. Excellent linearity and about 5 orders of magnitude dynamic range was demonstrated for the experimental set-up. Outstanding long term stability of the PDB technique was also utilized because the detection system was possible to keep stable for even several weeks for rubber membranes with extremely slow permeation process.

Our measurements provide reproducible and reliable information on permeation parameters of polymer sheets for natural gas and oil industry, where there are only limited experimental data available in the literature for extreme conditions.

Applications of photoacoustic resonances for soft matter characterization

S. Galović¹ ✉, M. Nešić¹, M. Popović¹, M.D. Rabasović², D. Markushev²


¹Vinca Institute of Nuclear Sciences, University of Belgrade, Belgrade, Serbia

²Institute of Physics, University of Belgrade, Belgrade, Serbia


✉ bobagal@vinca.rs

In this work, experimental photoacoustic measurements of soft matter samples have been presented, with resonant peaks occurring in the modulation range below 20 kHz. Classic model of the photoacoustic response does not predict the occurrence of resonant frequencies, so their presence was explained using generalized composite piston model. Also, the position of resonance peaks was demonstrated to depend on heat propagation speed through the sample. With this relation in mind, heat propagation speeds for several materials in use have been evaluated.

**Study on photoacoustic technique
of thermophysical properties of human skin**

A. Yoshida¹ , A. Imuta¹, T. Yamada¹, K. Kagata¹

¹Department of Mechanical Engineering, Osaka Prefecture University
1-1 Gakuen-cho, Naka-ku, Sakai, Osaka, 599-8531, Japan

 ayoshida@me.osakafu-u.ac.jp

In recent years, the technical methods related to the heat transfer phenomenon have been increasingly applied in the field of medical technology such as the laser treatment and the frozen operation. The necessity for accurately grasping thermophysical properties of the biological material has risen. The biological material functions in vivo, and then it is necessary to measure knowing the thermophysical properties accurately in vivo. In addition, because the physical properties are different according to the body part, the individual specificity, and the state, it is preferable that the properties are decided by the on-site measurement to each body part than are considered to be constant values. Handy, noninvasive and prompt measuring method is requested for the above-mentioned reasons.

The photoacoustic technique has the following features. (1) The measuring device is comparatively handy and prompt. (2) The nondestructive measurement is possible, because advance preparation and processing are not necessary for the measuring object. It is suitable for the measurement of the human body because of the above-mentioned points. However, the human skin is a material not handled easily by the current absorption spectroscopy because the scattering of light strengthens by wavelength. Therefore, in the present study, the photoacoustic measurements are carried out for the thermal effusivity and the thermal diffusivity of the skin in vivo by using the light of the wavelength with high absorption comparatively in the skin. When considering simulation model composed of sample, plate and gas shown in Fig.1, with thermal properties of opaque plate known, only thermal effusivity of sample can be measured [1]. Improving this disadvantage, opaque plate is replaced by semi-transparent one. The equation of photoacoustic signal is based on thermal diffusion equations. The difference of the phase of the photoacoustic signal to incident light is shown as follows as the

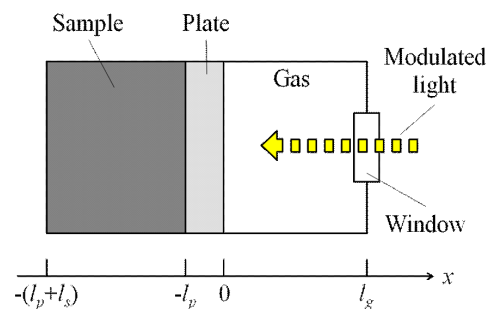



Fig. 1. Measurement model of photoacoustic method for double materials.

function of six parameters of thickness of plate, extinction coefficients of plate and sample, thermal diffusivity of plate and sample, and ratio of thermal effusivity of plate and sample. We measured thermophysical properties of a sample that properties are given for validation of the method. We used a rigid polyvinyl chloride (PVC) sheet as thin plate and an epoxy resin as sample. The result shows the present technique is sufficiently accurate. The measurements were carried out for thermal effusivity and then thermal diffusivity of human skin.

[1] A. Yoshida, K. Kagata, T. Yamada, *Int. J. Thermophysics*, **31**, 2019–2029, (2010)

Cavity enhanced absorption spectroscopy and photoacoustic spectroscopy for human breath analysis

J. Wojtas¹ , F.K. Tittel², T. Stacewicz³, Z. Bielecki¹, R. Lewicki², J. Mikołajczyk¹,
M. Nowakowski¹, D. Szabra¹, P. Stefański², J. Tarka²

¹Military University of Technology, Institute of Optoelectronics, 00-908 Warsaw, Poland

²Rice University, Electrical and Computer Engineering Department, Houston, TX 77005, USA

³University of Warsaw, Institute of Experimental Physics, 00-068 Warsaw, Poland

 jwojtas@wat.edu.pl

The paper describes laboratory setups of two highly sensitive optoelectronic techniques: cavity enhanced absorption spectroscopy (CEAS) and photoacoustic spectroscopy (PAS). The setups are designed for investigation of exhaled volatile compounds. The analysis of the human breath is useful for health monitoring. The presence of certain gases (biomarkers) at unusual concentrations in human breath might indicate many serious diseases.

At present, the volatile biomarkers are analyzed using various chemical tools: mainly gas chromatography, mass spectrometry or the chemiluminescence. Rising interest of application of optoelectronic methods is observed recently. Here laser techniques are of great potential for detection and monitoring of the chemical components in gas phase. While the simple setups employing so-called direct laser absorption spectroscopy technique attain a detection limit up to 10^{-4} cm⁻¹, the CEAS sensors provide a detection limit of about 10^{-9} cm⁻¹. In this technique, an optical cavity of a high quality factor is applied. The cavity is built of two concave highly reflective mirrors. This results in a long optical path, reaching even up to a few kilometers [1]. Similar detection limit can be achieved by use of photoacoustic spectroscopy. PAS is based on the conversion of light to sound in absorbing materials. The photoacoustic signal is traditionally detected using a resonant acoustic cell equipped with a sensitive microphone. The sensitivity of PAS can be increased many times due to the use of resonance quartz forks (QTFs) [2]. Such technique is called quartz-enhanced photoacoustic spectroscopy (QEPAS). The QEPAS based sensor platforms are characterized by a non-complex design, immunity to environmental acoustic noise, applicability over a wide range of pressures, and the capability to analyze small gas samples, down to 1 mm³ in volume.

Application of CEAS or PAS for biomarker monitoring provides opportunity to detect the pathogenic changes at molecular level. Because of non-invasive operation, easy use, the ability to

re-use, real time measurement, minimum nuisance for patients, these sensors might be very useful tools for health monitoring.

These works are supported by The National Centre for Research and Development (research project ID 179900.) and National Science Centre (research project No 2011/03/B/ST7/02544).

- [1] J. Wojtas, Z. Bielecki, T. Stacewicz, J. Mikolajczyk, M. Nowakowski, *Opto-Electron.* **20**, 77–90 (2012)
- [2] R.F. Curl, F. Capasso, C. Gmachl, A.A. Kosterev, B. McManus, R. Lewicki, M. Pusharsky, G. Wysocki, F.K. Tittel, *Chem. Phys. Lett.* **487**, 1–18 (2010)

Dynamics of thermal denaturation of blood proteins: study with photothermal methods

E. Sehn¹ ✉, G.V.B. Lukasiewicz², F. Sato², M.L. Baesso²

¹Núcleo de Física, Universidade Tecnológica Federal do Paraná, Medianeira, PR, Brazil

²Departamento de Física, Universidade Estadual de Maringá, Maringá, PR, Brazil

✉ elizandra@utfpr.edu.br

The photothermal techniques, in particular the photoacoustic spectroscopy, has been applied in analysis of biological systems such as permeation formulations in skin [1, 2], nail [3] and dentin [4], evidencing the importance of this technique for this area. Now, in this work, we applied photothermal methods, photoacoustic spectroscopies and thermal lens, allied to conventional techniques for employed to investigate the dynamics of thermal denaturation of blood proteins. The studies were performed in albumin, blood plasma and blood serum.

The results showed changes in the measured properties when the sample temperature was varied between 35 and 55 °C, which is the interval where proteins changes the conformational from native to denaturated phases. The combination of several methods allowed to perform an evaluation of the samples conformational changes, especially the decrease of the α -helix followed by the increase of the β -sheet structures, besides the formation of aggregates, detected in the absorbance data. The results, especially those obtained with the thermal lens technique showed, the occurrence of structural modifications that are difficult to detect via calorimetric methods, suggesting this technique as a new tool to study the conformational properties of proteins. In conclusion, this work showed through non-conventional methods the detection of the denaturation processes of blood proteins.

Finally, it was demonstrated, that the thermal lens and the photoacoust spectroscopy are new tools to study proteins denaturation processes, indicating that the adopted procedure can be used to investigate other animal and vegetal proteins, in order to correlate their thermal stability behavior with the conformational structures.

- [1] E. Sehn, L. Hernandez, S. L. Franco, C. C. M. Gonçalves, M. L. Baesso, *Anal. Chim. Acta* **635**, 115–120, (2009)

- [2] E. Sehn, K. C. Silva, V. S. Retuci, A. N. Medina, A. C. Bento, Rev. Sci. Instrum. **74**, 758–560 (2003)
- [3] A. M. Koroishi, E. Sehn, M. L. Baesso, T. Ueda-Nakamura, C. V. Nakamura, D. A. G. Cortez, B. P. Dias Filho, Molecules **15**, 3920–3931 (2010)
- [4] A. L. M. Ubaldine, M. L. Baesso, E. Sehn, F. Sato, A. R. Benetti, R. C. Pascotto, J. Biomed. Opt. **17**, 1–5 (2012)

Direct estimate of cocoa powder in cakes: colorimetry and photoacoustic approach

O. Dóka¹ ✉, R. Kulcsár², D. Bicanic³

¹University of West Hungary, Deák F. sq.1, 9200 Mosonmagyaróvár, Hungary

²PEZ Produktion Europe Kft., H-9241 Jánossomorja, Pez-Haas str.1, Hungary

³Wageningen University, Dreijenlaan 3, 6703 HA Wageningen, The Netherlands

✉ dokao@mtk.nyme.hu

Cocoa (*Theobroma cocoa L.*) is an important ingredient widely used in manufacturing industry and largely consumed worldwide [1]. One distinguishes two types of unsweetened cocoa powder: the natural and the Dutch-processed one. Natural cocoa is very dark, tart and acidic while Dutch cocoa powder undergoes an alkalization to neutralize the natural acids, a process that dramatically changes its color as well as the flavor. The change of color varies from a reddish-brown to almost black.

At present there exists no method capable of directly quantifying the content of cocoa powder in confectionary products. In practice, concentrations of caffeine and theobromine in such specimens are usually determined first and the content of cocoa computed using empirical formulas [2]. In the study described here, the potential of the photoacoustic spectroscopy (PAS) and colorimetry for a direct determination of cocoa powder content in cakes has been explored.

As a first step, one has manufactured a “basic (blank, raw) cake” thereby using ingredients such as hen egg, margarine, milk, wheat flour and baking powder. From this basic cake (that contained no cocoa powder) one has prepared six test samples by adding predetermined quantities of unsweetened Dutch cocoa powder. All samples were then baked in preheated oven (175 °C) for 30 min. Once cakes completely dried to a room temperature, they were grounded to a very fine powder and then sieved. Upon weighting each cake before baking and after the drying process, one could calculate the concentration of cocoa powder in dried cakes. Second series of test samples included three different commercially available cakes purchased from local supermarket. One of the cakes contained no cocoa powder whatsoever, while according to data reported on the product label, the content of cocoa powder in two other cakes was about 3%.

The home made PA spectrometer used in this study was described previously [3]. In addition to a continuously tunable Xe lamp emitting relatively low c.w. output power, Roithner GLP-III-532-30 diode laser was used as a strong, c.w. monochromatic (532 nm) radiation source. Because of a direct proportionality between the magnitude of the PA signal and incident power, the availability of a

strong radiation source will assist in obtaining better detection limits. Colorimeter MiniScan XE Plus was used to measure the color of test samples and the outcome expressed in the CIELAB color space in terms of colorimetric index L^* and total color difference (ΔE^*).

Both analytical methods provide satisfactory results. In case of self-made cakes the relationship between PAS signal and cocoa content was linear. On the other hand, the correlations between L^* and ΔE^* with cocoa content were quadratic. As far as commercially available cakes are being concerned, L^* and PAS both produced values close to a content reported on product's label while the measurement of ΔE^* yielded the cocoa content slightly below that expected.

[1] M. Rusconi, A. Conti, *Pharmacol. Res.* **61**, 5–13 (2010)

[2] A. Richards, B. Wailes, *J. Assoc. Public. Anal.* **40**, 1–12 (2012)

[3] O. Dóka, D. Bicanic, M. Bunzel, *Anal. Chim. Acta.* **514**, 235–239 (2004)

Photoacoustic quantification of food colorants in confectionery

O. Dóka¹ ✉, R. Kulcsár², D. Bicanic³, Zs. Ajtony¹

¹University of West Hungary, Deák F. sq.1, 9200 Mosonmagyaróvár, Hungary

²PEZ Produktion Europe Kft., H-9241 Jánossomorja, Pez-Haas str.1, Hungary

³Wageningen University, Dreijenlaan 3, 6703 HA Wageningen, The Netherlands

✉ dokao@mtk.nyme.hu

Next to flavor and nutritional value color is one of the most important quality attributes of foods. Increased appeal of attractively colored foods usually means increased consumption. Food colorants can be classified divided in three groups, namely natural colorants, synthetic colorants and colorants from natural origin. The number of commercially available colorants currently exceeds several thousands but their legal application as food additives is under strict regulations. Several compounds are either believed to cause cancer, or are toxic if consumed in excessive quantities [1]. In this study two colorants (one natural and from natural origin), namely the betanin (E162) and the sulphite ammonia caramel (E150d), were investigated in food supplements. E162 is a red/purple natural coloring agent, derived from beetroots and approved by the European Union. It may contain nitrates and should therefore not be consumed by infants and young children. E150d which is made by controlled heat treatment of sugar with ammonia and sulphite containing compounds can have colour ranging from dark brown to black. It can be found in several foods.

High pressure liquid chromatography, column chromatography, thin-layer chromatography and capillary electrophoresis are currently often used to separate, identify and quantify colorants. Besides these methods, traditional spectrophotometry is used as well. This latter without the use of chemometrics yields accurate analytical data only when a single colorant is present in foods [2]. In addition, direct quantification can be accomplished only if the sample to be analyzed is presented as a clear, transparent liquid.

The intent of the study described here was to explore the feasibility of laser PA spectroscopy for a direct quantification of E162 and E150d in powdered multivitamin tablets and candies. As a first

step a “basic” sample (without food dyes) was prepared from vitamins, saccharine, sugar, etc. according to the composition of the products. After this, different series of samples were prepared by adding varying amounts of E162 and E150d to the basic sample. Laser photoacoustics (PA) was then used with these samples construct the calibration curves.

Traditional spectrophotometry was applied to obtain spectra of the above mentioned colorants. E162 exhibits a strong and wide absorption at 520 nm while the absorbance of E150d is decreases steadily from the UV to the end of the visible range. The PA cell and the spectrometer used here were described previously [3]. The CW532-04-30mW and a MBL-III-473-50mW lasers emitting at 532 nm and at 473 nm were used as radiation sources. The wavelength of green laser (532 nm) is close to the maximal absorbance of betanin. The blue laser (473 nm) on the other hand gives higher signal from E150d than green one, this is to higher power and larger absorption coefficient.

Constructed calibration curves were used to quantify the amount of colorants in commercially available samples (multivitamin tablets, candies). In both cases measured PA signals are linearly proportional to the content of food colorants. The obtained results are satisfactory for both food colorants.

- [1] K.C. Chen, J.Y. Wu, C.C. Huang, Y.M. Liang, S.C.J. Hwang, *J. Biotechnol.* **101**, 241–252 (2003)
- [2] P.L. López-de-Alba, K. Wróbel-Kaczmarczyk, K. Wróbel, L. López-Martínez, J.A. Hernández, *Anal. Chim. Acta* **330**, 19–29 (1996)
- [3] O. Dóka, G. Ficzek, D. Bicanic, R. Spruijt, S. Luterotti, M. Tóth, J. G. Buijnsters, Gy. Végvári, *Talanta*. **84**, 341–346 (2011)

Direct quantification of carotenoids in low fat baby foods via laser photoacoustics and colorimetric index a*


O. Dóka¹ , Zs. Ajtony¹, D. Bicanic², D. Valinger³, Gy. Végvári⁴

¹University of West Hungary, Deák F. sq.1, 9200 Mosonmagyaróvár, Hungary

²Wageningen University, Dreijenlaan 3, 6703 HA Wageningen, The Netherlands

³University of Zagreb, Savska c. 16, HR-10000, Zagreb, Croatia

⁴Corvinus University of Budapest, Villányi str. 29-43, 1118 Budapest, Hungary

 dokao@mtk.nyme.hu

Carotenoids, natural pigments synthesized by plants and many microorganisms, are responsible for vibrant colors of many flowers and fruits. This is of particular relevance for foods because their color, often a criterion of quality, is affected by the processing. The content of carotenoids in fruits and vegetables depends on several factors such as genetic variety, maturity, postharvest storage, processing etc. In addition, carotenoids are important due to their nutritional and health properties. Some carotenoids are not only precursors of vitamin A but act as antioxidants as well. As to the human health, carotenoids were shown effective in lowering the incidence of some cancers, reducing the risk of heart disease etc.

This study explores the analytical potential of laser photoacoustic spectroscopy (PAS) and reflectance colorimetry (TC) to quantify total carotenoid content (TCC) of baby foods. Well established optical spectrophotometry (SP) served as a reference method. Unlike SP, the PAS and TC require no extraction prior to the analysis and permit rapid assessment of TCC after only one initial calibration step.

Five jars of commercially available baby foods (A, B, C, D, E) were obtained from local supermarket. Samples A and B contain carrot and first fruits carrot respectively. Pumpkin is a major constituent of sample C, while tomato and potato dominate in sample D. Finally, sample E is composed of apple, pumpkin and apricot (E). All samples contained little fat; and were not pre-cooked, but pureed to a reasonably homogenous consistency.

The spectrometer Spectroquant Pharo 100 (Merck) was used to record spectra of all samples between 400 and 600 nm. Hexane (pro anal), acetone (pro anal), absolute ethanol (pro anal) and β -carotene (purity>97%) were all purchased from Merck Millipore (Hungary). Extraction of carotenes was achieved using the slightly modified procedure described by Markovic et al. [1]. The PA cell and the spectrometer used here were discussed previously [2]. The MBL-III-473-50mW laser emitting 50 mW c.w. power at 473 nm served as a light source. MiniScan XE Plus colorimeter was used to measure the color of the samples and the outcome expressed in the CIELAB color space in terms of basic colorimetric indices (L^* , a^* and b^*). Quantities such as the total color difference ΔE^* and chroma C^* , both calculated from measured L^* , a^* and b^* were also discussed.


The TCC in baby foods was expressed in terms of β -carotene equivalents. The highest TCC (21.2 mg/100 g fresh product weight) was found in A as compared to a lowest TCC value (4.3 mg/100g) for sample E. Positive linear correlation between food color and TCC was established only for index a^* . Increasing TCC in 100 g fresh product by one mg results in 77 μ V increment of PA signal and 0.85 larger a^* units. In conclusion, both PAS and TC proved excellent methods for a low cost, simple and rapid assessment of carotenoids in functional foods such as low fat baby foods.

- [1] K. Markovic, I. Panjkota Krabavcic, M. Krpan, D. Bicanic, *Acta Aliment. Hung.* **39**, 90–98 (2010)
- [2] O. Dóka, G. Ficzek, D. Bicanic, R. Spruijt, S. Luterotti, M. Tóth, J.G. Buijnsters, *Gy. Végvári, Talanta* **84**, 341–346 (2011).

Laser photoacoustic method in dendrochronology: 300-years CO₂ chronology of annual tree rings

B.G. Ageev, Yu.N. Ponomarev , V.A. Sapozhnikova

V.E. Zuev Institute of Atmospheric Optics SB RAS
Acad. Zuev Square 1, 634021 Tomsk, Russian Federation

 yupon@iao.ru

The effect of atmospheric CO₂ increase on plant and, in particular, on forests has been studied for many decades already. The climate change (CO₂ increase and temperature rising) might lead a

considerable growth intensification, but this not the case often. We think that this can be clarified by studying the annual CO₂ in disc tree rings. Early we had shown efficiency of photoacoustic (PA) gas-analyser with tunable wave-guide CO₂ laser for detection of CO₂ emission by plants, including CO₂ content in disc tree ring [1, 2]. Spectral range of CO₂ laser tuning is 925–1088 cm⁻¹, the threshold gas concentration detected by gas-analyser is 180 ppm.


The laser photoacoustic gas-analyser is unique in that it can not only trace the annual CO₂ trend in discs but also characterize the H₂O distribution over tree rings. The wood of tree rings are placed in four sealed exposure chambers pumped out for a short time to stimulate sorbed gas diffusion and gas concentration was detected using (PA) gas-analyzer. We have measured the annual CO₂ distribution in every tree ring of fir (*Abies sibirica* Ledeb.), spruce (*Picea obovata* Ledeb.), Siberian stone pine (*Pinus sibirica* Du Tour), and Scots pine (*Pinus sylvestris* L.) tree discs taken from the forests near Tomsk, West Siberia and Siberian stone pine tree discs from the Altai Mountains. The span of our analysis was up to 300 years for Siberian larch. To verify the fact that CO₂ in the samples studied was generated by the tree itself and not supplied from the atmosphere, an isotope analysis of the carbon ($\delta^{13}\text{C}$) CO₂ for a few rings was performed. Correlation analysis of annual CO₂ distributions in disc tree rings with climatic parameters was made.

Thus, the use of the laser photoacoustic method provides a unique opportunity for study the multiyear time series of the CO₂ and H₂O contents in conifer disc tree rings and studying valuable information on their relation to atmospheric parameters.


This work is supported by Project VIII.80.1 of Basic Research Program of SB RAS.

- [1] B.G. Ageev, Yu.N. Ponomarev, V.A. Sapozhnikova, Applied Physics B. **67**, 467–473 (1998)
- [2] B.G. Ageev, Yu.N. Ponomarev, V.A. Sapozhnikova, Sensors **10**, 3305–3313 (2010)

Investigation on plant pathogen interaction by LPAS sensor

A. Puiu, G. Giubileo , A. Lai

ENEA Frascati, Via E. Fermi 45, 00044 Rome, Italy

 gianfranco.giubileo@enea.it


The plants use different defence mechanisms to protect themselves from many biotic aggressors attack, both pathogens and insects. Signaling molecules as ethylene (ET) are involved in the systemic plant resistance. By monitoring the plants ET, it is possible to obtain useful information about plant-pathogen interaction. The ethylene has biological activity at very low concentration, order of 10⁻⁹ M at 25°C, and a very high sensitivity detector is required to detect ethylene from a single plant. The laser photoacoustic spectroscopy (LPAS) technique offers an accurate solution to perform high sensitivity trace gas detection (typically under 1 ppbv) for small molecules and posses a time resolution of only a few minutes.

A homemade laser sensor realised at ENEA Frascati (Italy), based on the laser photoacoustic spectroscopy in the infrared spectral region, able to detect gas concentrations down to ppb level, was


applied for monitoring ethylene traces emitted by plants in stress condition. In the present work, the biotic stress response of tomato mutant plants after inoculation with *Phthorimaea operculella* larvae (*Lepidoptera*: Gelechiidae) was investigated with the a.m. LPAS sensor. The photoacoustic setup, the methods and the experiments are described; the results are discussed.

IMAGING

Cluster segmentation of thermal image sequences using kd-tree structure

R. Świta , Z. Suszyński

Koszalin University of Technology, Multimedia Systems and Artificial Intelligence Department,
Śniadeckich 2, 75-453 Koszalin, Poland

 robert.swita@wp.pl

This article presents the cluster image segmentation method, adapted to process a sequence of thermal images. Images of the sample response in the frequency domain to thermal stimulation with a known spectrum were subjected to cluster segmentation, grouping pixels with similar frequency characteristics. Segmentation of the entire sequence to a single image enables determination of the depth profile parameters of the materials based on a small number of characteristics and in fact practical implementation of thermal tomography of materials.

The sample in a result of thermal excitation gives us response we can study both in the time and frequency domain. The sequence of images will contain different information in each frame, depending on the internal structure of the sample. Changes in the frames are continuous, therefore we can talk about the characteristics of each pixel of the image. To reduce the data processing one can use the cluster segmentation, which has a well-defined error and allows for an objective quality comparison of the various methods used for this purpose. It is quite rare feature of the segmentation algorithms. The easiest and most popular cluster segmentation algorithm is k-means, which is an iterative method. Program performs in each iteration image posterization, by assigning pixels to the nearest segment center values. Before proceeding to the next iteration the segment centroids are recalculated on the average of all the pixels belonging to the segment. The algorithm always converges, but because it may coincide with some time to a local minimum, one often stops it at the time of crossing the threshold of minimal change between iterations. Clustering is a per pixel segmentation, depending only on the value of the pixel and does not take into account the value of neighboring pixels. This information can, however, be included in the image by using statistical or low-pass filtering before segmentation.

This paper presents optimization method for the k-means segmentation algorithm of a sequence of thermal images with kd-tree algorithm [1] that divides the set of the pixels to the subspaces in the hierarchy of binary tree. This allows skipping the calculation of distances of pixels to some centroids and seeding set of centroid clusters through the hierarchy tree. Dimension reduction of the segmented data has also been applied. Compared are not individual pixels, but all the pixel characteristics in the function of frame number by minimizing the sum of deviations of the pixel from their segments mean of all the frames of processed image sequence. Results of the speed and accuracy of the segmentation were compared with the k-means and FCM algorithm MATLAB implementations. FCM cluster

algorithm [2] assumes that the pixels can belong to segments with a specific weight and in general it finds a better solution, but paid for increased computational effort, and hence, a longer processing time.

- [1] T. Kanungo, D.M. Mount, N.S. Netanyahu, C.D Piatko, R. Silverman, A.Y Wu, IEEE Trans. Pattern Anal Machine Intel. **24**, (2002)
- [2] G. Hamerly, Ch. Elkan, Proc. ACM Conf. Inform. Knowl. Management (CIKM), 600–607 (2002)

Photoacoustic signal formation in heterogeneous multi-layered systems with piezoelectric detection

M.V. Isaiev¹ , D.A. Andrusenko¹, A.G. Kuzmich¹, V.V. Lysenko², R. Burbelo¹

¹Faculty of Physics, Taras Shevchenko National University of Kyiv,
64/13, Volodymyrska Street, City of Kyiv, Ukraine, 01601

²Institut des Nanotechnologies de Lyon (INL), UMR-5270, CNRS, INSA de Lyon,
Universite de Lyon,
bat. Blaise Pascal, 7 Av. Jean Capelle, Villeurbanne 69621, France

isaev@univ.kiev.ua

Photoacoustic (PA) techniques are successfully applied for multi-scale investigations of various physical parameters of heterogeneous materials. In particular, PA methods based on piezoelectric detection allow simultaneous evaluation of thermal and elastic parameters of complex structures. However, different incomplete theoretical approaches developed for PA signal description are very cumbersome for express experimental data analysis required for numerous practical applications.

We will report on a new efficient model describing PA signal formation with piezoelectric detection. We consider the following multi-layered sandwich-like systems (see Fig. 1) defined as: heterogeneous studied structure – buffer layer – piezoelectric transducer. In these systems, the buffer layer is used for spatial redistribution of thermoelastic force moments generated in the investigated structure. Thus, mechanical properties of this layer play a crucial role to ensure perfect control of the detected voltage formed on piezoelectric transducer by contribution of different regions of the studied structure. In particular, formation of the voltage signal strongly

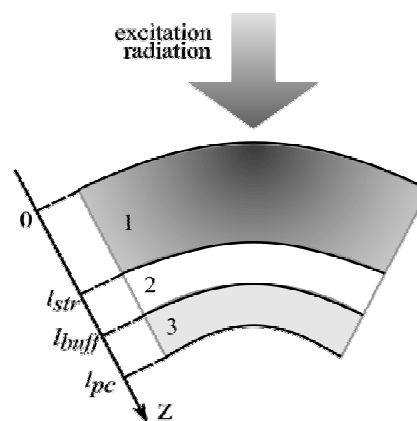


Fig. 1. Schematic view of the used multi-layered sandwich-like system: (1) – heterogeneous studied structure; (2) – buffer layer; (3) – piezoelectric transducer.

depends on a point at which thermo-elastic source is applied. Therefore, the use of relatively simple linear Green's functions introduced in frames of Kirchhoff-Love theory is chosen as an efficient approach for the PA signal description.

Moreover, excellent agreements between the theoretical model and measured results obtained on heterogeneous "porous silicon – bulk Si substrate" structure is stated. Furthermore, resolving of the inverse problem with fitting of the experimental curves by the developed model allow reliable simultaneous evaluation of: (i) thermal conductivity of the nanostructured porous silicon layer, (ii) thermal resistance of the interface between the porous layer and bulk substrate and (iii) elastic properties of the whole system.

Photoacoustic imaging of defects in MEMS

N. Chigarev¹ ✉, C. Ni¹, V. Tournat¹, O. Bou Matar², V. Gusev³

¹LAUM, UMR-CNRS 6613, Université du Maine, Av. O. Messiaen, 72085 Le Mans, France

²LICS / LEMAC, IEMN CNRS 8520, Ecole Centrale de Lille, Villeneuve d'Ascq 59651, France

³IMMM, UMR-CNRS 6283, Université du Maine, Avenue O. Messiaen, 72085 Le Mans, France

✉ Nikolay.Chigarev@univ-lemans.fr

The control of reliability of Micro-Electro-Mechanical Systems (MEMS) is important for micro-electronics. Contactless laser photoacoustic technique looks very promising for nondestructive evaluation and characterization of MEMS. In our previous work [1,2], this technique has been successfully validated on the natural crack initiated in the light-absorbing glass of cm dimension. In the present work, this technique is applied to detection of an artificial nanometric crack, produced in MEMS using focused ion beam technology (FIB).

The acoustic vibration of the cantilever covered by nanometric metallic film is excited by the absorption of the first pump cw laser beam modulated in amplitude in range 0.1–100 MHz (Fig. 1). Then, the vibration is detected by photo-deflection technique with a knife introduced before the photodetector in a probe cw laser beam. The photoacoustic signal is processed by a spectrum analyzer. Second pump laser beam, modulated in range 0–10 kHz, is focused on the surface of sample to change the state of the crack by local increase of the temperature. The thermoelastic strain induced by the heating could close the crack to provide corresponding change in the spectrum of vibration of the cantilever. By studying the spectrum of photoacoustic signal during a scan of pump beam along the sample surface, the image of a crack could be obtained. The space resolution of $\sim 5 \mu\text{m}$ is mostly controlled by the size of the laser spots on the surface. Photoacoustic method allows the quantitative characterization of cracks in MEMS.

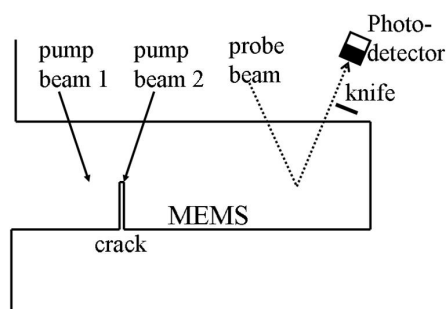



Fig. 1. Experimental configuration for photoacoustic imaging of a crack in MEMS.

Moreover, the photoacoustic experiment with the artificial defect with controlled parameters, produced by FIB, should help to improve the theory of nonlinear frequency mixing in the crack. [3]

This research is supported by the grant ANR-10-BLAN-092302.

- [1] N. Chigarev, J. Zakrzewski, V. Tournat, V. Gusev, J. Appl. Phys. **106**, 036101 (2009)
- [2] S. Mezil, N. Chigarev, V. Tournat, V. Gusev, Opt. Lett. **36**, 3449–3451 (2011)
- [3] V. Gusev and N. Chigarev, J. Appl. Phys. **107**, 124905 (2010)

Advantages and disadvantages of thermal measurements using spatial modulation technique

M. Kosikowski , Z. Suszyński

Koszalin University of Technology, Faculty of Electronics and Computer Science,
Śniadeckich 2, 75-453 Koszalin, Poland

 mateusz.kosikowski@tu.koszlin.pl

Flying Spot thermography (known also as Beam Displacement Modulation) is a common technique for fast visualization of defects in electronic devices. The method basis on a scanning technique with a continuous wave laser excitation and IR point detector. Designed thermal wave microscope for fast visualization of thermal non-uniformities in solids using flying spot technique is presented in Fig. 1. It consists in exciting the object with a constant energy value of the focused optical radiation witch moves when compared to the object. The highest efficiency of detecting thermal inhomogenities may be obtained for the excitation and detection in the broad band of the frequency spectrum.

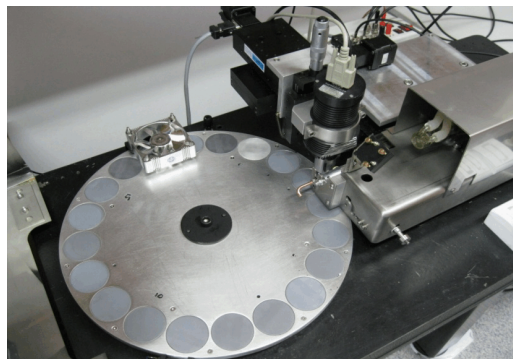


Fig.1. Measurement setup.

The information on the thermal properties of the object is derived from measuring the thermal response in the excitation area or in its vicinity. The infrared detector is situated so as to record temperature changes with a certain delay after the excitation. Due to complexity of the measurement system the parameters of the device, which influence the measurements, have to be chosen properly by means of the thermal impedance of scanned objects. The main advantages of BDM method are the broadband frequency spectrum of excitation. It allows observing thermal properties on variant depths. Relatively short time required for the measurements is another advantage of presented method. Disadvantage of the method is that the recorded images have to be

processed in order to proper visualization of thermal non-uniformities. The article discusses the concept of acquisition and processing of thermal images recorded in the mode of spatial modulation. The basic problem related to analyzing thermal images acquired in such a way is the inhomogeneity of the thermal background and significant diversification of signal levels, stemming from optic contrast differences. In the beam displacement modulation mode, the temperature signal value is recorded for successive pixel for the same lag when compared to the excitation which for large optical contrast differences brings about significant discrete signal changes with a finite relaxation time, resulting in linear signal distortion, visible as trails in the images.

Photothermal measurements by the use of scanning thermal microscope

J. Bodzenta¹ ✉, J. Juszczyk¹, A. Kaźmierczak-Bałata¹, G. Wielgoszewski²

¹Institute of Physics-CND, Silesian University of Technology,
B.Krzywoustego 2, 44-100 Gliwice, Poland

²Faculty of Microsystem Electronics and Photonics, Wrocław University of Technology,
Z. Janiszewskiego 11/17, 50-372 Wrocław, Poland

✉ Jerzy.Bodzenta@polsl.pl

The scanning thermal microscope (SThM) is a useful tool for temperature measurement with high sensitivity and high spatial resolution. The idea of utilizing SThM in photothermal (PT) experiment

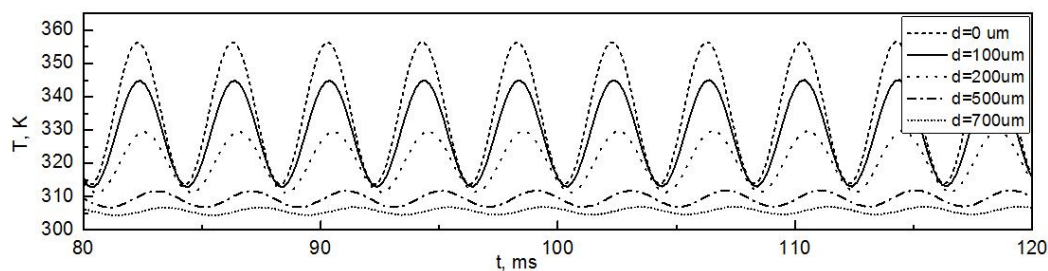


Fig. 1. Evolution of temperature in a few points selected at sample surface.

was examined both numerically and experimentally. Firstly a model of PT experiment with a sample illuminated by tightly focused light beam was created using finite element method. It was assumed that impinging angle is of about 60° . The light was intensity modulated. Time dependent temperature field in the sample was analyzed. An evolution of temperature in a few points selected at sample surface along a straight line perpendicular to the symmetry plane of a system was shown in Fig. 1. Calculations were carried out for silicon. Amplitude and phase of ac temperature component were

determined in further analysis. Dependence of these quantities on distance from the symmetry plane for two modulation frequencies are shown in Fig. 2 a) and b).

To verify results of numerical analysis a module allowing illumination of the sample was installed in the SThM and appropriate experiment was carried out. The sample was heated by the intensity modulated light from laser diode ($\lambda = 830$ nm). Temperature of the sample surface was measured using nanofabricated thermal probe driven by relatively low current (0.3 mA) to avoid additional probe and sample heating. Probe voltage was analysed by lock-in amplifier (SR 830, SRS) and the amplitude and the phase of ac temperature component was determined. An exemplary experimental data measured for Poco Graphite (NETZSCH) reference sample are shown in Fig. 2 c). Qualitative agreement between numerical predictions and experiment was obtained.

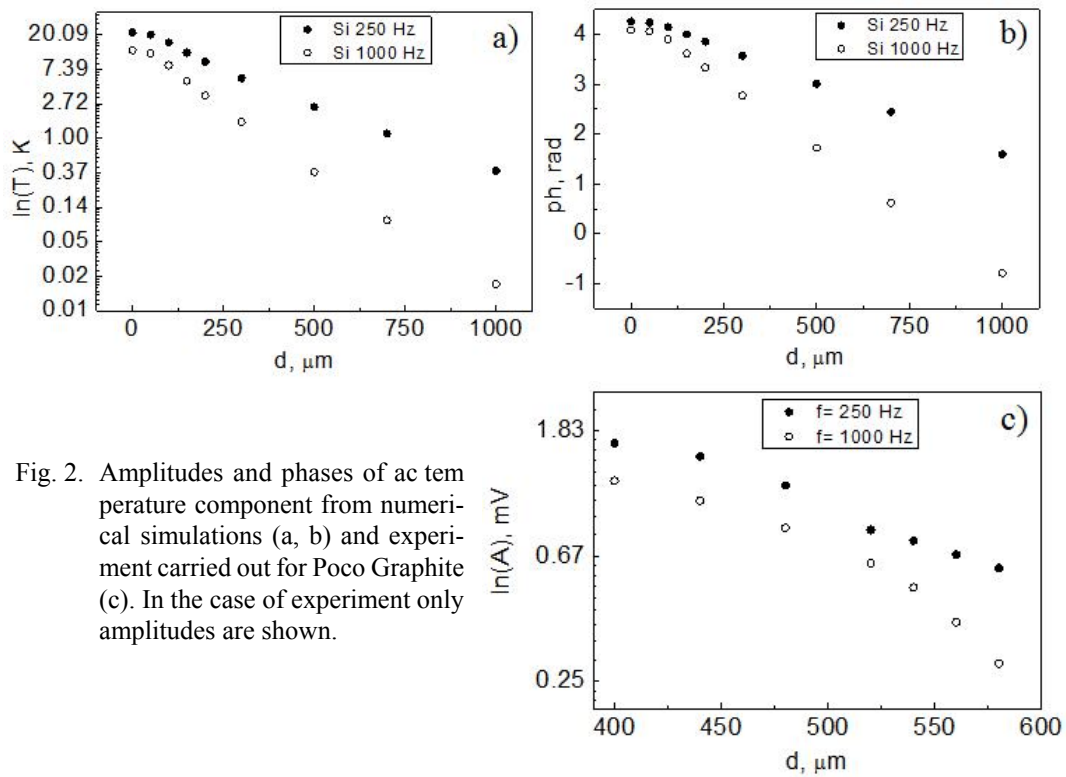


Fig. 2. Amplitudes and phases of ac temperature component from numerical simulations (a, b) and experiment carried out for Poco Graphite (c). In the case of experiment only amplitudes are shown.

ULTRAFAST, MICRO/NANOSCALE AND NONLINEAR PHENOMENA

Nanoscale magnetic characterization by SThM-modulated ferromagnetic resonance

P. Kijamnajsuk^{1,a}, R. Meckenstock¹, M. Chirtoc², J. Pelzl³ 

¹Department of Physics, AG Farle, University Duisburg-Essen, Germany

²Equipe de Caracterisation Thermophysique Multiechelle, GRESPI-ECATHERM UFR
Sciences, Moulin de la Housse, BP 1039 51687 Reims, France

³Institute of Experimental Physics VI, Ruhr-University, Bochum, Germany

 josef.pelzl@rub.de

Ferromagnetic resonance (FMR) offers a very sensitive tool for the measurement of fundamental magnetic parameters. The FMR method is based on the absorption of microwaves by magnetic moments which undergo a precessional motion in a static external field. As the whole sample contributes to the resonance the conventional signal cannot provide spatially resolved information. To overcome this drawback one can take advantage of the temperature dependence of the resonance. Thermal waves are induced locally by a laterally confined external heat source. As a result the microwave resonance absorption at the heated area is temperature modulated and can be monitored by the microwave bridge at the modulation frequency. This method has been successfully implemented by using a focused intensity modulated laser beam as heat source offering lateral resolutions on microscale. To extend the lateral resolution into the submicron range we applied the tip of the scanning thermal microscope (SThM) as a local heater. The ferromagnetic film was positioned inside a rectangular microwave cavity below the upper cover plate with hole in it to enable the contact between the film and the tip of the SThM. The present studies were conducted with a commercial SThM equipped with a Wollaston tip (Fig.1). The sample was a 20 nm thick film of iron epitaxially grown on a GaAs substrate. The ferromagnetic signal of iron was recorded as a function of the external magnetic field at a fixed microwave frequency of 9.2 GHz.

In this work we have undertaken a detailed study of the SThM-modulated signal as a function of the modulation frequency, the ac-heating current of the tip and the distance between the tip and the sample. The microwave response was recorded at the fundamental ($1f$) and the first harmonic ($2f$) of the ac-current and compared with the conventionally measured FMR signal. In addition, the $3w$ -signal from Wollaston tip was studied as a function of the modulation frequency.

Resonance signals of the aligned and not-aligned mode of iron were observed at $1f$ and $2f$. The $1f$ signals are due to electrical perturbation of the cavity resonance. At $2f$ two different kinds of

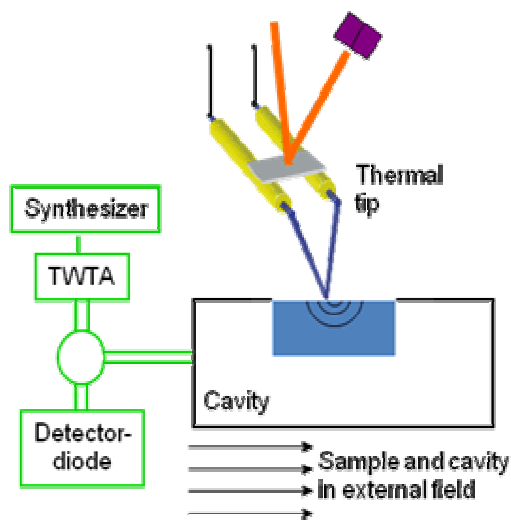



Fig. 1. Experimental set-up for the SThM-modulated ferromagnetic resonance.


resonances appear. One kind exhibits a strong decrease with modulation frequency as it is expected for thermally modulated resonance absorption. The second kind of resonance detected at $2f$ is restricted to the not-aligned mode excitation and shows no dependence on modulation frequency. This resonance is found to arise from a local modulation of the magnetic field produced by the Wollaston tip and can only be observed when magnetization and external field have different orientations. When the tip is lifted from the sample surface the thermally modulated resonance signal does not vanish immediately proving that there is heat conduction via air contributing to the thermally modulated resonance signal. The problem is modeled by finite element simulation with a curved line source in the air layer above the sample surface.

a) On leave from Department of Physics, Kasetsart University, Bangkok 10900, Thailand

Acoustic waves generation in a transparent matrix by host metal nanoparticle illuminated by laser pulses

N.I. Grigorchuk 

Bogolyubov Institute for Theoretical Physics, Kyiv, Ukraine

 ngrigor@bitp.kiev.ua


The theory of the photo-acoustical effect caused by a laser action on metal nanoclusters embedded in a dielectric matrix is built [1]. The energy absorbed by clusters propagates through the dielectric matrix and generates the sound waves in it via the thermo-deformation mechanism. The formulae for an acoustical signal are derived, and the high sensitivity of the sound wave amplitude to the shape of metal clusters, as well to such parameters of a laser irradiation as the frequency, polarization, and intensity, is revealed. The behavior of the sound vibrations amplitude in a region of the surface plasmons absorption is studied in detail. In particular, we obtain that this amplitude in a spheroidal MNs as a function of the frequency of a laser beam has two maxima of different intensities, in contrast to the spherical MNs, where a single maximum is observed. By the distance between the doublet peaks, we can estimate the degree of oblateness or prolateness of MN. The intensity of the doublet peaks can be controlled by the variation of the incidence angle of a laser

beam relative to the rotation axis of a spheroid. It is found, as well, that this amplitude at light absorption by a discrete metal film (a system of clusters in the matrix) can exceed the corresponding amplitude for the absorption by a continuous metal film in the region of plasmon resonances by several orders of magnitude.

An approach has been proposed for the generation of acoustic oscillations in a dielectric medium by small-sized spherical metallic nanoparticles illuminated by ultrashort laser pulses [2–4]. Analytic expressions have been derived for the amplitude and power of the longitudinal spherical acoustic oscillations as functions of the density and elastic properties of the medium, the laser pulse duration, electron temperature, particle radius, and electron-phonon coupling constants. The dependence of the maximum displacement of the oscillator during the excess pressure “shock” by the electron gas on the shear modulus and the density of the material in the metallic nanoparticles has been found. It is shown that, besides being determined by the “impact” of the electron pressure, the power of the acoustic wave is determined by the rates of cooling of the electron gas and its pressure variation. The magnitude of the pressure of the acoustic signal at the end of the laser pulse can be used to estimate the maximum electron temperature in the metallic nanoparticle. The total energy of the acoustic oscillations of a metallic nanoparticle in a specified medium has been determined. The efficiency with which the energy of the hot electrons is removed by acoustic oscillations has been examined for a number of metals. It has been shown that the acoustic energy transfer efficiency is considerably higher in media with low shear moduli. The factors affecting the damping dynamics of the power of acoustic waves are studied in detail for the cases of Au, Ag, and Cu metallic nanoparticles embedded in a plexiglas matrix. In particular, the way the electron-phonon coupling in these materials affects the removal of the electron energy through acoustic oscillations is studied. An illustration is provided of the dynamics of the oscillations in the acoustic power as a function of nanoparticle radius.

- [1] N.I. Grigorchuk, P.M. Tomchuk, *Eur. Phys. J. B.* **80**, 371–378 (2011)
- [2] Y. Bilotsky, N.I. Grigorchuk, P.M. Tomchuk, *Surf. Sci.* **603**, 3267–3274 (2009)
- [3] Y. Bilotsky, N. Grigorchuk, P. Tomchuk, M. Gasik, *J. Phys.: CS.* **214**, 012050 (2010)
- [4] N.I. Grigorchuk, *Low. Temp. Phys.* **80**, 329–336 (2011)

Photoacoustic discrimination of optical absorbers based on non-linear generation

A. Prost, O. Simandoux, J. Gâteau, E. Bossy 

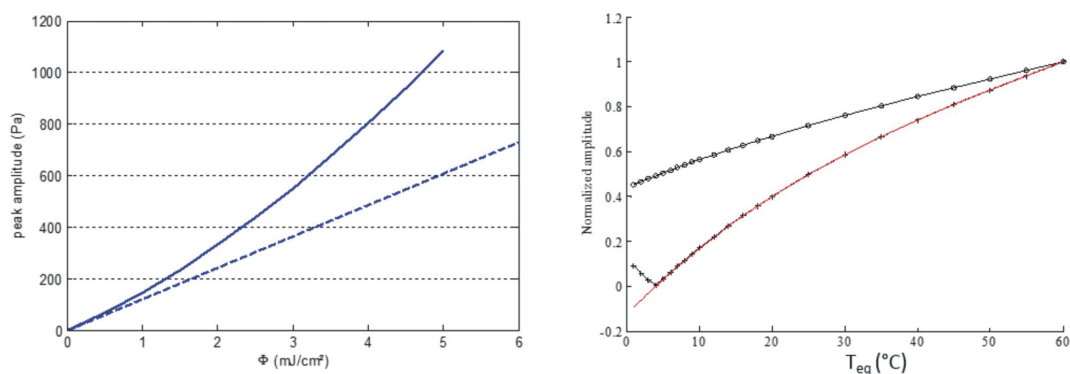
Institut Langevin, ESPCI ParisTech, CNRS UMR 7587, INSERM ERL U979
1 rue Jussieu, 75005 Paris, France

 emmanuel.bossy@espci.fr

Photoacoustic imaging relies on the detection of ultrasound waves generated by the absorption of light via thermo-elastic effects. While endogenous absorption in tissue may by itself provide contrast for photoacoustic imaging, various exogenous contrast agents have been extensively studied

either for contrast enhancement or for molecular imaging. The objective of the theoretical and experimental work reported here is to demonstrate that the photoacoustic response of a contrast agent may under appropriate conditions be highly dependent on the nature of that contrast agent. Under such conditions, the conventional assumption that photoacoustic signals are dependent only on the distribution of absorbed energy breaks down.

In a theoretical study by Diebold *et al.* [1], it was shown analytically that point source absorbers may yield a non-linear dependence of the photoacoustic signal with the illumination fluence. The predicted non-linearity was caused by the temperature-dependence of the thermal expansion coefficient β , which may become significant if the fluence is high enough. In the current work, photoacoustic signals are predicted for various contrast agent (molecular dyes, gold nanoparticles, graphite particles), taking into account several parameters including their size and absorption properties, as well the exact temperature-dependence of the β coefficient for water. The predictions are based on a semi-analytical solution the heat diffusion problem and on a FDTD (finite-difference time-domain) solution of the photoacoustic wave equation.



The figure shows two typical predictions: on the left, the photoacoustic amplitude is plotted as a function of fluence, for a 40-nm diameter gold nanosphere immersed in water at room temperature (dashed line: linear contribution only). On the right, the photoacoustic signal amplitude is plotted as a function of the equilibrium temperature, for a fixed fluency: the crosses corresponds to the prediction for a molecular dye, the circles to that for nanoparticles. The red curve plots the dependence of β with temperature. These predictions are in agreement with experimental results (not show here). The contribution of the non-linearity (left, full line) strongly depends on the equilibrium temperature, which provides a way to discriminate various type of absorbers. Applications to selective imaging will be presented and discussed.

[1] I. Calasso, W. Craig, G. Diebold, Phys. Rev. Lett. **86**, 3550–3553 (2001)

THERMOPHYSICS

Complementary photothermal techniques for complete thermal inspection of solids

D. Dadarlat¹ , M. Streza¹, O. Onija¹, K. Strzałkowski², C. Prejmerean³, D. Prodan³,
L. Silaghi-Dumitrescu³, N. Cobirzan⁴

¹National Institute for Research and Development of Isotopic and Molecular Technologies,
65-103 Donáth Str., 400293 Cluj-Napoca, Romania

²Institute of Physics, Faculty of Physics, Astronomy and Informatics,
Nicolaus Copernicus University, Grudziądzka 5, 87-100 Toruń, Poland

³"Raluca Ripan" Institute for Research in Chemistry, 400294, Cluj-Napoca, Romania

⁴Technical University of Cluj Napoca, Faculty of Civil Engineering, Department of Civil
Engineering and Management, 25 G. Baritiu Street, 400027, Cluj-Napoca, Romania

 ddadarlat@gmail.com

The paper is focused on the ability of combining photothermal techniques for complete thermal characterization (measurement of all thermal parameters) of solid samples. A contact technique (photopyroelectric (PPE)) and a non-contact one (IR thermography (T)) have been combined for thermal characterization of various solids (semiconductors, dental filling polymers, drugs, building materials).


It is well known that almost all photothermal techniques are able now to perform a complete characterization of a solid sample, if the requirements of the particular detection cases are fulfilled. Usually the photothermal methods allow the direct measurement of thermal diffusivity and effusivity; the remaining thermal parameters can be then calculated. However, in order to measure the dynamic thermal parameters mentioned before and to obtain particular detection cases of experimental interest, one has to perform some theoretical/experimental optimizations by acting especially on the number of layers and on the optical and thermal thickness of each layer of the detection cell. For the contact techniques, a perfect sensor/sample thermal contact is also crucial.

On the other hand, the solid materials under investigation present sometimes particularities acting against the requirements of the particular detection cases: they are transparent or present rough surfaces, they can be obtained only as very thin layers or opposite, only as bulk samples, the coupling fluid (contact techniques) can penetrate inside the sample, etc. Consequently, sometimes it is necessary to combine different techniques for a complete characterization of the material. Several attempts have been already successfully reported; we cite here, as example, a contact (PPE)-noncontact (PTR) approach [1, 2].

In this paper we will combine a contact technique (PPE) with a non-contact one (T) in order to investigate some "special" samples as composite materials used in dentistry, drug industry and buildings, and some semiconductors. The composition and the geometry of the investigated samples make the PPE method (in "front" detection configuration together with TWRC technique as scanning procedure) suitable for thermal effusivity measurements and the lock-in thermography for thermal diffusivity investigations. In such a way, this combination leads to a complete thermal characterization of the materials.

- [1] D. Dadarlat, M. N. Pop, M. Streza, S. Longuemart, M. Depriester, A. Hadj Sahraoui, V. Simon, *Int. J. Thermophysics*, **31**, 2275–2281 (2010)
 [2] D. Dadarlat, M. N. Pop, M. Streza, S. Longuemart, M. Depriester, A. Hadj Sahraoui, V. Simon, *Int. J. Thermophysics*, **32**, 2092–2101 (2011)


Temperature dependence of optical absorption in defect chalcopyrite semiconductor CdGa_2Te_4 studied by photoacoustic spectroscopy

B.K. Sarkar¹ , A.S. Verma², S. Sharma², P.S. Deviprasadh³

¹ Department of Physics, Galgotias University, Greater Noida-201308, India

² Department of Physics, Banasthali Vidhyapith, Rajasthan 304022, India

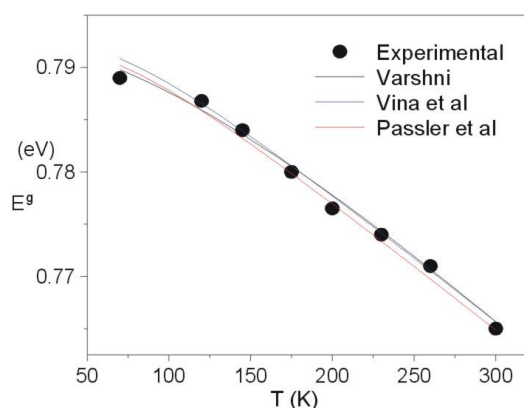
³ Department of Physics, CMS College of Engineering & Technology, Coimbatore 641032, India

 bks@physics.org.in

We have presented the temperature dependent optical absorption in defect chalcopyrite semiconductor CdGa_2Te_4 ($\text{A}^{\text{II}}\text{B}_2^{\text{III}}\text{C}_4^{\text{VI}}$) in the temperature range from 70 to 300 K by photoacoustic spectroscopic method. Optical-absorption has been measured for this defect-chalcopyrite-type semiconductor as a function of photon-energy. The thermal variation of band-gap energy (E_g) has been estimated from the optical-absorption spectra.

Electron-phonon interaction explained the temperature variation of bandgap for CdGa_2Te_4 . Varshni's empirical relation in conjunction with Vina and Passler model has been taken in consideration for data fitting. We have also explained the band-gap shrinkage effect in CdGa_2Te_4 .

The change of band gap as a function of temperature results from two contributions, thermal expansion [1] and the renormalization of the electronic energies due to electron-phonon interaction [2]. In our work the band gap shrinkage has been explained based on electron-phonon interaction [3].



The Debye temperature was determined as 190K. The acoustic phonons with a characteristic temperature as 220 K corresponding to effective mean frequency have been attributed to the thermal variation of the band gap.

- [1] J. Malloy, K. J., Van Vechten, J. A., J. Vac. Sci. Technol. B. **9**, 2212–2218 (1991)
- [2] Camassel, J., Auvergne, D., Phys. Rev. B. **12**, 3258–3267 (1975)
- [3] Zoliner, S., Gopalan, S., Cardona, M., Solid State Commun. **77**, 485–488 (1991)

Photoacoustic elastic bending method: study of the microcantilevers

D.M. Todorović¹ , D.D. Markushev², M.D. Rabasović², V. Jović³, M. Sarajlić³

¹Institute for Multidisciplinary Researches, University of Belgrade, Belgrade, Serbia

²Institute of Physics, University of Belgrade, Belgrade-Zemun, Serbia

³Institute for Chemistry Technology and Metallurgy, Belgrade, Serbia

dmtodor@afrodita.rcub.bg.ac.rs

The photoacoustic (PA) and photo-thermal (PT) science and technology extensively developed new methods for the investigation of micromechanical structures. The PA and PT effects can be important also as driven mechanisms for optically excited micromechanical structures. The photoacoustic elastic bending method (PA-EBM) is based on the optical excitation of the micromechanical structure and detection of the acoustic response (PA signal) with a very sensitive PA detection system.

The basic concept, development and application of the PA-EBM are presented. The amplitude and phase of the PA elastic bending signals vs. the modulation frequency of the excitation optical beam for various types of micromechanical structures (the cantilevers, the membranes, the thin plate, etc.) were measured and analyzed.

The PA-EBM enables to investigate the optical, electronic, thermal and elastic characteristics for different micro-

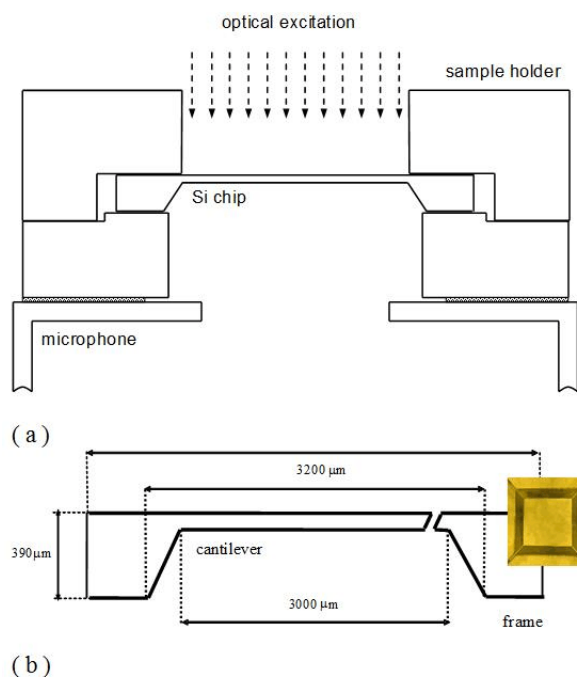


Fig. 1. Photoacoustic elastic vibration method: a) cross-section of the PA cell with the sample (Si – chip 5 x 5 mm with glass cover); b) cross-section and dimension of the Si – chip with rectangular cantilever (without the glass cover).

electro-mechanical-structures (MEMS). The PA elastic bending spectra of the optically driven MEMS enable also to investigate the different technological processes in MEMS fabrications, etc.

The experimental PA elastic bending signals of the whole micromechanical structure were measured by using special constructed PA cell (the gas-microphone detection technique with transmission configuration). The PA amplitude and phase spectra were measured, as a function of the modulation frequency in a frequency range from 20 to 20000 Hz, for different samples of microstructures (Si chip with square membrane, microcantilever, etc).

The plasma, thermal and elastic waves, i.e. the carrier-density, temperature and elastic displacements, distribution in a micromechanical structures, photogenerated by an intensity-modulated optical beam, are analyzed. The relations for thermodiffusion, thermoelastic and plasmaelastic components of the PA signal are given. The characteristics of the microcantilever were quantitatively investigated by comparing the experimental and calculated theoretical PA elastic bending signals.

Measurement of the thermal parameters of selected II-VI crystals by means of photopyroelectric methods and infrared lock-in thermography

K. Strzałkowski¹ ✉, D. Dadarlat², M. Streza², A. Marasek¹

¹Institute of Physics, Faculty of Physics, Astronomy and Informatics, Nicolaus Copernicus University, Grudziądzka 5, 87-100 Toruń, Poland

²National R&D Institute for Isotopic and Molecular Technologies, Donath Str. 65-103, POB-700, 400293 Cluj-Napoca, Romania

✉ skaroll@fizyka.umk.pl

The II-VI semiconductors are very promising materials largely used as visible radiation sources in green laser diodes, in spintronics, photodetection and other applications in modern optoelectronics [1]. From the application point of view, the main feature of the ternary and quaternary II-VI compounds, is the possibility of smooth change of the band gap and lattice constant values [2].

The crystals under investigation have been grown from the melt by the high pressure high temperature modified Bridgman method. Crystal rod was cut into the plates of about 1 mm thickness, then the samples were mechanically grinded, polished and chemically etched in NaOH water solution.

Thermal diffusivity is a very important parameter characterizing the energy dissipation in miniaturized semiconducting devices. It is a unique parameter for each material, strongly dependent on the composition and structural characteristic of the sample. For the investigated semiconductors the thermal diffusivity was experimentally obtained by two methods: (i) the photopyroelectric (PPE) technique [3] in back detection configuration and (ii) by contactless infrared imaging technique using fast infrared FLIR camera with lock-in detection. Thermal effusivities of the same semiconductors were obtained by using PPE technique in front configuration (FPPE), coupled with thickness (TWRC-thermal wave resonator cavity) and frequency scanning procedures.

It is well known that the four thermal parameters (thermal diffusivity, effusivity, conductivity and volume specific heat) are connected by two relationships and consequently, the measured thermal effusivity and thermal diffusivity allowed to calculate the thermal conductivity of the investigated materials. The thermal parameters have been determined as a function of composition of mixed ternary and quaternary II-VI crystals.

- [1] Y. Niiyama and M. Watanabe, *Semicond. Sci. Technol.* **20**, 1187 (2005)
- [2] F. Rozpłoch, J. Patyk, F. Firszt, S. Łęgowski, H. Męczynska, J. Zakrzewski, A. Marasek, *Phys. Stat. Sol. (b)* **229**, 207 (2002)
- [3] A. Mandelis, M.M. Zver, *J. Appl. Phys.* **57**, 4421 (1985)

Investigation of the influence of rolling on the thermal diffusivity of metal alloys by photothermal infrared radiometry

I. Delgadillo-Holtfort^{1,2}, B.K. Bein², P. Kijamnajsuk^{2,a}, M. Chirtoc³, J. Pelzl² 

¹Instituto de Física de la Universidad de Guanajuato, IFUG, Apdo. E-143 León, Gto., Mexico

²Institut fuer Experimentalphysik, Ruhr-Universitaet, D-44801 Bochum, Germany

³Multiscale Thermophysics Lab. GRESPI-CATHERM, Université de Reims Champagne-Ardenne URCA, Moulin de la Housse BP 1039, 51687 Reims, France

 josef.pelzl@rub.de

The thermal diffusivities of metallic foils subjected to cold-rolling processes have been studied by photothermal infrared radiometry (PTR). The PTR measurements were conducted on foils of Al, Cu and stainless steel (V2A). The starting thickness of the metallic foils was 1 mm. By successive cold-rolling processes the thickness was reduced stepwise down to 0.1 mm. The thermal diffusivity of the untreated and mechanically treated foils was investigated at room temperature with frequency dependent PTR in thermal transmission and reflection configuration. Thermal waves were excited by an argon-ion laser beam of 600 mW which was intensity-modulated with the help of an acousto-optical modulator in the frequency interval between 0.1 Hz and 10 kHz. For the normalisation of the signal flat discs of glassy carbon and of Ta were used.

The amplitude and phase of the PTR response was analyzed in the frame of a one-dimensional heat transport model consisting of a one layer sample with air backing. The change of the foil thickness d due to cold-rolling was determined with a digital micrometer. Across the measured area the thickness of the sample was constant within a range of about $\pm 5\%$. In Fig. 1 the obtained diffusivity values for the stainless steel sample are plotted versus the logarithm of the relative thickness d/d_0 where d_0 is the thickness of the untreated foil and d that of the rolled sample. Rolling reduces considerably the thermal diffusivity α . For the stainless steel foil the diffusivity decreases linearly with the logarithm of the relative thickness. Also cold rolled foils of Al and Cu obey within the error bars a linear dependence of α with the logarithm of d/d_0 . These observations differ from the

results obtained on NiTi foils, which exhibit a linear dependence of α on d/d_0 . The effusivity e determined from PTR phases measured in thermal reflection is also reduced by rolling comparable to that of α .

The observed behavior of α and e as a function of the degree of rolling is attributed mainly to the generation of internal interfaces by the mechanical treatment. Rolling increases the number of dislocations and grain boundaries. This leads to an increase of the contribution of the interfaces to the overall thermal resistance of the foil. A model is presented that is based on a one-dimensional heat flow perpendicular to the foil surface. The thermal resistances of the interfaces and that of the grains are considered to be in series. Due to rolling the size of the grains perpendicular to the surface is assumed to decrease proportional to the thickness of the foil. To explain the observed dependences on the relative thickness also a change of the thermal conductivity and specific heat density of the grains has to be taken into account.

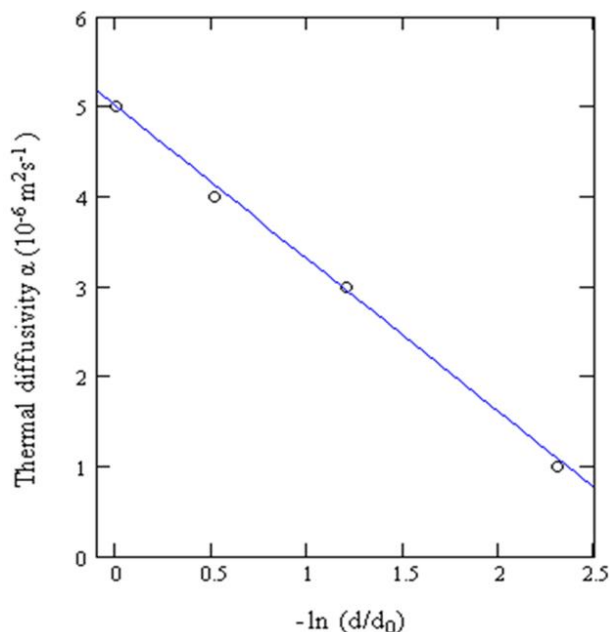



Fig. 1. Change of the thermal diffusivity α of stainless steel foil as a function of the logarithm of the relative thickness d/d_0 .


^{a)} On leave from Department of Physics, Kasetsart University, Bangkok 10900, Thailand

Photothermoelastic characterisation of a tuning fork used in infrared and photoacoustic spectroscopy

M. Spajer¹ , S. Euphrasie¹, B. Cavalier¹, X. Vacheret¹, D. Vernier¹, G. Matten¹, P. Vairac¹, A. Jalocha²

¹ FEMTO-ST, Université de Franche-Comté, CNRS, ENSMM, UTBM, 25044 Besançon cedex, France

² CILAS, Departement de Photonique, 8 av. Buffon - BP 6319, 45000 Orléans, France

 michel.spajer@univ-fcomte.fr

Quartz tuning fork (QTF) has proved to be efficient sensors in photo-acoustical spectroscopy [1] as well as in absorption spectroscopy of solid pollutants (thin layer, powder...) [2]. The setup of

this second application is depicted by Fig.1. Fig.2 shows the evolution of the piezoelectric signal of the QTF while a CO₂ laser beam scans a grid of carbon black deposited on a metallic surface. The signal maximums are consistent with the presence of carbon black. The main purpose of our study is to elucidate the physical origin of the signal and to characterize precisely the spatial variations of the fork sensitivity. We assume that the excitation comes from the mechanical strain due to the local heating by the CO₂ laser beam reflected on the sample. To better understand the phenomena, experiments were made in the visible domain ($\lambda=670$ nm) with the QTF vacuum encapsulated: a tenfold enhancement of the signal and of the Q factor is obtained.

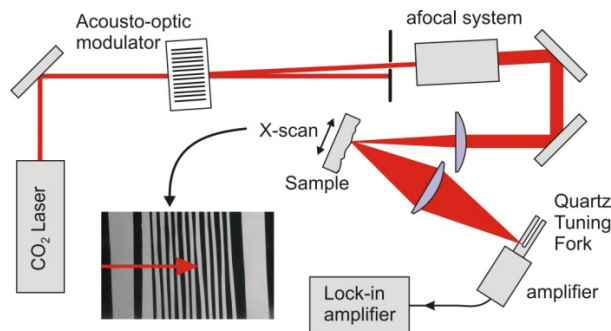


Fig.1. Set-up of the absorption measurement in the reflection configuration.

Besides, Fig.3 presents the piezoelectric response of the QTF during its complete XY-scan by the laser spot. The main feature is the black line (null signal) which, according to our hypothesis, should follow the line of minimum strain. This is confirmed by the simulated volume strain mapping (Fig.4), at least in the two prongs area. This mechanical model will be improved by taking into account the piezoelectric and thermal properties of the QTF.

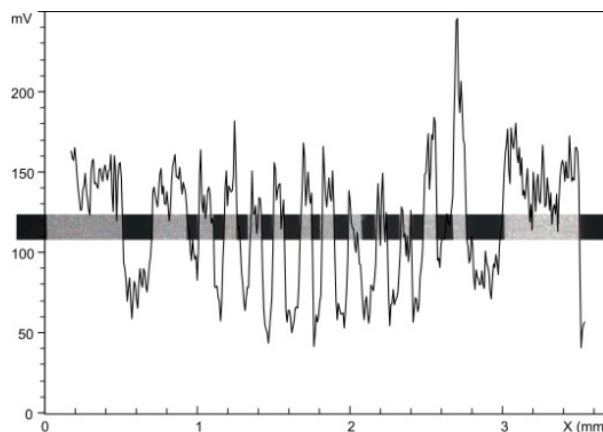


Fig. 2. Piezoelectric signal evolution during a single scan.

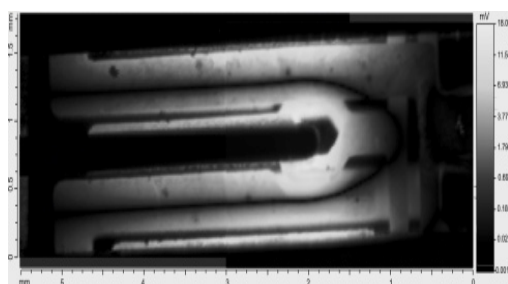



Fig. 3. Piezoelectric signal mapping from a scan of the QTF.



Fig. 4. Simulation of the volume strain of the quartz tuning fork.

- [1] N. Petra, J. Zweck, A.A. Kosterev, S.E. Minkoff, D. Thomazy, Appl. Phys. B **94**, 673–680 (2009)
- [2] C. W. Van Neste, L. R. Senesac, T. Thundat, Appl. Phys. Lett. **92**, 234102 (2008)

Photothermal study of the effect of thermal annealing on the thermal interface resistance of Cu-coated carbon and Cu-coated diamond

N. Horny¹, J. Hell², M. Chirtoc¹, P. Kijamnajsuk^{3,a}, C. Eisenmenger-Sittner², J. Pelzl⁴ 

¹Multiscale Thermophysics Lab. GRESPI-CATHERM, Université de Reims Champagne-Ardenne URCA, Moulin de la Housse BP 1039, 51687 Reims, France

²Vienna University of Technology, Institute of Solid State Physics, Wien, Austria

³Department of Physics, AG Farle, University Duisburg-Essen, Germany

⁴Institute of Experimental Physics VI, Ruhr-University, Bochum, Germany

 Josef.pelzl@rub.de

Modern materials such as nano-composites are based on coated fibers or particles in order to benefit from the particular physical properties of the constituents. Carbon fibers or small crystals of diamond coated with a copper films promise superior mechanical properties combined with high thermal and electrical conductivities. However, in the composite material due to the large number of interfaces the thermal and electrical interface resistance between the two constituents is similarly important. As the packetizing of the constituents mostly occurs at higher temperature the effect of thermal annealing on the interface resistance will also have an important impact on the material properties.

In this work we have investigated copper coated carbon substrates and small diamond crystals by photothermal infrared radiometry (PTR). Measurements were conducted as a function of modulation frequency on as prepared and thermally treated samples. The copper-carbon samples consisted of a 2 mm thick glassy carbon substrate on which Cu films were deposited by magnetron sputtering. By the same method small diamond crystals with diameter of 5 mm and a thickness of 2 mm were also coated with copper. For both types of substrates samples with Cu-coating thicknesses of 200 nm, 500 nm, 800 nm and 1300 nm were prepared. One half of the samples were subjected to a heat treatment under argon atmosphere at 800°C.


The amplitude and phase of the PTR-signal were measured in the frequency ranges from 1 kHz to 100 kHz for the copper-carbon samples and in the range 100 kHz to 1 MHz for the copper-diamond samples. The frequency ranges were selected to allow data analysis by a one-dimensional heat transport model. The as-measured data were normalized with the signals from uncoated carbon.

The variation of the amplitude and phase data as a function of the different thicknesses of the Cu coating offered a means to deduce a reliable value of the thermal interface resistance R_{th} that did not depend on the normalization procedure. The as-prepared copper-carbon samples exhibit a mean R_{th} value of $2 \cdot 10^{-7} \text{ m}^2\text{KW}^{-1}$. The thermal annealing did not change markedly the resistance values between copper and carbon. For the as-prepared copper-diamond samples with copper layers 800 nm

and 1300 nm thickness the thermal interface resistance is one order of magnitude smaller than those of the copper-carbon samples. On heat treatment these values increased up to one order of magnitude. The observations from the as-prepared samples are explained by a stronger bonding of the Cu-atoms on the nearly perfect surface of the diamond crystals as compared to that on the rougher carbon substrate. On thermal treatment the large difference of the thermal expansion coefficients of Cu and substrate most probably leads to partial lifting of the Cu-film on diamond whereas in the case of the carbon substrate the rough surface weakens the effect of mismatch.

^{a)} On leave from Department of Physics, Kasetsart University, Bangkok 10900, Thailand


Correlation between the Hall carrier concentration and the effective IR optical absorption coefficient in CdMgSe mixed crystals measured by the photothermal IR-radiometry

M. Pawlak¹ , M. Maliński², F. Firszt¹, J. Pelzl³, A. Wieck³, A. Marasek¹

¹ Institute of Physics, Nicolaus Copernicus University, Grudziądzka 5/7, Toruń, Poland

² Department of Electronics and Computer Science, Koszalin University of Technology, Śniadeckich 2, Koszalin 75-453, Poland

³ Experimental Physics VI, Ruhr-University Bochum, 44780 Bochum, Germany

 mpawlak@fizyka.umk.pl

In this work we demonstrate the ability to determine the level of carrier concentration in semiconductors by a photothermal infrared radiometry (PTR) experiment. The present measurements were conducted on Cd_{1-x}Mg_xSe crystals which are semi-transparent in the infrared wavelength range. Mixed single crystals were grown by high-pressure Bridgman method without a seed under an argon overpressure. The PTR experiments were conducted at room temperature in thermal reflection and transmission configurations. An intensity modulated argon-ion laser beam was used as a heat source and a MCT detector to register the infrared radiation. The amplitude and phase of the PTR signal were measured as a function of the modulation frequency in the range 1 Hz to 100 kHz. The PTR data were analyzed in the frame of a one-dimensional heat transport model. Thermal and optical parameters were obtained from the numerical simulation of the frequency variation of the normalized PTR phase and amplitude. The normalization procedure utilizes the PTR signal measured in the transmission and reflection configuration. In the normalized PTR (NPTR) approach, for infrared semi-transparent samples, the signal can be written as follows [1,2]

$$NPTR \sim \frac{\int_0^L \beta_{IR} \Delta T(z) e^{-\beta_{IR}(L-z)} dz}{\int_0^L \beta_{IR} \Delta T(z) e^{-\beta_{IR}(z)} dz} \quad (1)$$

where $\Delta T(z)$ is the temperature distribution perpendicular to the surface given by Malinski [3], L is the sample thickness, β_{IR} the effective IR absorption coefficient. β_{IR} represents the infrared absorption

coefficient averaged over the wavelength range of the MCT detector. From the numerical analysis of experimental data and using formula (1) the values of the thermal diffusivity and the effective absorption coefficient were determined. The obtained values of the thermal diffusivities agree well with those determined by means of the photopyroelectric technique from the same crystals [4]. The effective IR absorption coefficients β_{IR} for different compositions are compared with the Hall carrier concentration measured independently on the same crystals. The obtained linear dependence relation of the effective IR absorption coefficient β_{IR} and the carrier concentration is discussed in the frame of the Drude theory.

- [1] H. G. Walther, U. Seidel, W. Karpen, and G. Busse, *Rev. Sci. Instrum.* **63**, 5479 (1992)
- [2] A. Mandelis, A. Othonos, C. Christofides, and J. Boussey-Said, *J. Appl. Phys.* **80**, 5332 (1996)
- [3] M. Maliński, *Arch. Acoust.* **27**, 217 – 228 (2002)
- [4] M. Pawlak, F. Firszt, S. Łęgowski, H. Męczyńska, J. Gibkes, J. Pelzl, *Int. J. Thermophys.* **31**, 187–198 (2010)

Modelling of the thermoacoustic frequency characteristics for the air-tightness test method

M. Kubicki, M. Maliński ✉

Department of Electronics and Computer Science
Koszalin University of Technology, Śniadeckich 2, 75-453 Koszalin, Poland

✉ mirosław.malinski@tu.koszalin.pl

The paper deals with the comparison of the two theoretical models describing the frequency amplitude and phase thermoacoustic characteristics. This is the essential issue from the point of view of the numerical interpretation of the experimental frequency amplitude and phase thermoacoustic characteristics observed for a series of packagings of transistors. Considerations of this type are essential also from the point of view of the theoretical determination of the sensitivity of the thermoacoustic method applied for the measurements of the air-tightness of the packagings of electronic elements. In the paper two models of the thermoacoustic signal are presented, described and discussed: CRC and CRLC. Both models were applied for the interpretation of the experimental frequency amplitude and phase thermoacoustic characteristics and the fittings to the experimental amplitude and phase frequency characteristics, obtained for a series of packagings, were performed and compared. The fittings were performed for the following transistor packagings: TO-3, TO-39 and TO-18. Additionally a method of extraction of the signal, coming from the hole in the packaging, from the total thermoacoustic signal of the packaging, is presented and discussed. It is illustrated with the computations performed on real experimental characteristics. Predictions of the model, concerning the sensitivity of this method of detection of the air tightness, applied for the series of electronic packagings, and the comparison of the theory with the experimental data is also shown and discussed.

Investigation of thermal properties of SiC ceramics containing carbon nanostructures by photothermal measurements

A. Kaźmierczak-Bałata¹ ✉, J. Bodzenta¹, J. Mazur²

¹Institute of Physics-CND, Silesian University of Technology,
Krzywoustego 2, Gliwice 44-100, Poland

²Institute of Nonferrous Metals, Sowińskiego 5, Gliwice 44-100, Poland

✉ akazmierczak@polsl.pl

In this work several silicon carbide ceramics containing different carbon nanomaterials (graphene flakes, carbon nanotubes) were examined. The samples were produced by the classical, two stages sintering method. Firstly samples were sintered at temperatures under 1400°C and under pressure of 25 MPa and then the pressure was doubled and temperature increased over 1400°C. Obtained samples differ in the density and composition.

The thermal diffusivity was determined by continuous wave photothermal technique with photoacoustic and IR detections. Both types of measurements were carried out in transmission geometry. The signal was measured at the sample surface opposite to illuminated one. In the first case the sample closed a PA cell and the PA signal was measured as a function of modulation frequency. In the second case the IR radiation from the sample surface was registered by IR detector. In both cases a dependence of signal phase on frequency was used to determine the sample thermal diffusivity.

Thermal properties are correlated with sample composition and density. The lower density corresponds to higher values of the thermal diffusivity, furthermore addition of carbon nanomaterials significantly improved thermal properties of investigated ceramics.

Analysis of the piezoelectric photothermal spectra of ZnSe, Zn_{1-x-y}Be_xMg_ySe and Zn_{1-x-y}Be_xMn_ySe crystals after different surface treatment

M. Maliński¹ ✉, J. Zakrzewski¹, K. Strzałkowski², F. Firszt²

¹Department of Electronics and Computer Science, Technical University of Koszalin,
Śniadeckich 2, 75-453 Koszalin, Poland

²Instytut Fizyki, Uniwersytet Mikołaja Kopernika, Grudziądzka 5/7, 87-100 Toruń, Poland

✉ mirosław.malinski@tu.koszalin.pl

The paper presents experimental and theoretical piezoelectric photothermal (PPT) spectra of several samples: ZnSe, Zn_{1-x-y}Be_xMg_ySe and Zn_{1-x-y}Be_xMn_ySe for the beryllium content x=0.05. The PPT spectra were measured for each group of samples after different surface treatment i.e. grinding,

polishing and etching. Considerable changes of the PPT amplitude spectra and small changes in the PPT phase spectra, observed after each step of the surface treatment, were next interpreted in a proposed model of a mechanically damaged surface layer. In this model, the layer exhibits a much smaller value of the Young's modulus than the bulk of the crystal.

The experimentally observed changes in the PPT amplitude and phase spectra were interpreted by the increase of the micro hardness of the crystals with the Be content. The paper also presents predictions of the proposed numerical model of the PPT signal for different thickness of a damaged surface layer as a function both of the energy of absorbed photons and also as a function of the optical absorption coefficient. The possibility of the measurement of the thickness of a surface damaged layer is also discussed from the point of view of a potential possibility of a determination of the best technology of surface preparation of semiconductor samples e.g. after ion implantation.

NAME INDEX

Ageev	55	Filep	38
Ajtai	38	Filus	46, 47
Ajtony	53, 54	Firszt	76, 78
Andrusenko	59	Franko	19, 21
Angster	26	Frez	17
Astrath	16, 22, 23, 40	Galović	48
Baesso	23, 51	Gâteau	66
Barrientos Barria	34	Geras	27, 28
Bein	72	Giubileo	41, 56
Bialkowski	16	Gladilin	42
Bicanic	52-54	Glière	45
Bielecki	50	Godard	34
Bodzenta	62, 78	Gong	36
Borowski	29	González	33
Bossy	66	Griffin	36
Bou Matar	60	Grigorchuk	65
Boutami	45	Gulyas	44
Bozóki	38, 44, 46, 47	Gusev	43, 60
Bruhns	30	Hell	75
Brun	45	Herculano	23, 40
Bulou	43	Hess	18
Burbelo	59	Horny	75
Burd	29	Imuta	49
Cavalier	73	Isaiev	59
Chigarev	43, 60	Jacinto	23
Chirtoc	64, 72, 75	Jahjah	36
Cobirzan	68	Jalocha	73
Czarny	45	Jiang	36
da Silva	26	Jović	70
Dadarlat	68, 71	Juszczuk	62
Delgadillo-Holtfort	72	Kapitanov	39
Deviprasadh	69	Każmierczak-Bałata	62, 78
Dherbecourt	34	Kijamnajsuk	64, 72, 75
Diebold	17	Korte	21
Dóka	52-54	Kosikowski	61
Dudkowiak	37	Kotkowiak	37
Egerev	42	Kottmann	13, 49
Eisenmenger-Sittner	75	Kowar	23
Euphrasie	73	Kubicki	77

Kulcsár	52, 53	Rouxel	45
Kuzmich	59	Santiago	33
Lai	56	Sapozhnikova	55
Lane	36	Sarajlić	70
Lefebvre	34	Sarkar	69
Lewicki	36, 50	Sato	51
Liu	19	Sehn	51
Lomonosov	18	Sharma	69
Lukasiewicz	16, 23, 51	Sigrist	13
Lysenko	59	Silaghi-Dumitrescu	68
Malacarne	22, 23, 40	Simandoux	66
Maliński	76-78	Slezak	33
Mami	24	So	36
Marasek	71, 76	Spajer	73
Marianovich	30	Stacewicz	50
Markushev	48, 70	Starecki	27-29, 31
Matten	73	Stefański	36, 50
Mazur	78	Streza	68, 71
Meckenstock	64	Strzałkowski	68, 71, 78
Melkonian	34	Suchenek	25, 29, 30
Mellouki	24	Suszyński	25, 58, 61
Miklós	26	Świta	58
Mikołajczyk	50	Szabó	38, 44
Nešić	48	Szabra	50
Ni	60	Talbot	36
Nicoletti	45	Tarka	36, 50
Nikitin	43	Tatrai	44
Nowakowski	50	Thomazy	36
Onija	68	Tittel	36, 50
Ovchinnikov	42	Todorović	70
Palucci	41	Tóth	46, 47
Parvitte	45	Tournat	60
Pawlak	76	Utry	38
Pelzl	14, 64, 72, 75, 76	Vacheret	73
Pereyra	33	Vairac	73
Peuriot	33	Valinger	54
Ponomarev	39, 55	Vallespi	33
Popović	48	Vallon	45
Prejmerean	68	Varga	44
Prodan	68	Végyvári	54
Prost	66	Verma	69
Puiu	41, 56	Vernier	73
Rabasović	48, 70	Walther	45
Raybaut	34	Wieck	76
Rey	13	Wielgoszewski	62
Robak	37	Wojtas	50

Wolff	30	Zbysiński	31
Wu	17	Zéninari	45
Yacoubi	24, 49	Zerr	43
Zakrzewski	78	Zhang	36
Zanuto	23		